PMM/C-69

Comisión Nacional de Energía Atómica
dependiente de la Presidencia de la Nación

CRITICAL POTENTIALS FOR LOCALIZED CORROSION OF ALUMINUM ALLOYS

J. R. Galvele, S. M. de De Micheli, I. L. Müller, S. B. de Wexler and I. L. Alanis.

PROGRAMA MULTINACIONAL DE METALURGIA
Programa Regional de Desarrollo Científico y Técnico-OEA

U. R. Evans International Conference on Localized Corrosion
6-10 December 1971, Williamsburg, Virginia.

DEPARTAMENTO DE METALURGIA
Buenos Aires-Argentina

PMM/C-69

Comisión Nacional de Energía Atómica
dependiente de la Presidencia de la Nación

CRITICAL POTENTIALS FOR LOCALIZED CORROSION OF ALUMINUM ALLOYS

J. R. Galvele, S. M. de De Micheli, I. L. Müller, S. B. de Wexler and I. L. Alanis.

PROGRAMA MULTINACIONAL DE METALURGIA
Programa Regional de Desarrollo Científico y Técnico-OEA

U. R. Evans International Conference on Localized Corrosion
6-10 December 1971, Williamsburg, Virginia.

DEPARTAMENTO DE METALURGIA
Buenos Aires-Argentina

CRITICAL POTENTIALS FOR LOCALIZED CORROSION OF ALUMINUM ALLOYS

J. R. Galvele, S. M. de De Micheli, I. L. Müller, S. B. de Wexler and I. L. Alanis

ABSTRACT

The present paper describes research work in progress in the Department of Metallurgy at the Atomic Energy Commission of Argentina. Emphasis was put on the mechanism of pitting initiation and its relation to stress corrosion cracking. The work done on aluminum and aluminum-copper alloys is described in detail, but results on iron and zirconium alloys are also reported.

Pitting

The pitting processes of aluminum in different electrolytes was studied. The influence of the composition of the electrolyte on the pitting morphology was considered. Emphasis was put on the fact that hemispherical brightened pits are not the rule and that etched-surface pitting can also be obtained in the high potential passivity breakdown.

Intergranular corrosion

The mechanism of intergranular corrosion of Al-Cu alloys was studied. It was found that intergranular corrosion of this alloy only occurs at potentials high enough to produce the passivity breakdown of a solute-depleted zone along the grain boundaries. Considerations about the difference between a solute-depleted zone and the precipitate-free zone in these alloys are made.

Stress-corrosion cracking

A good correlation between pitting potentials and the critical potential for stress corrosion cracking was found. The possibility of the existence of a single electrochemical mechanism in both processes is discussed.

Anodic behavior of yielding metals

The method of potentiostatic metal yielding was applied to aluminum and Al-Cu alloys to study their scc mechanism. The results obtained show a close correlation between the processes of scc and pitting. The application of the yielding metal method as a technique to study the mechanism of pitting processes is described.

Potential-Anion concentration diagrams

Determination of these diagrams, initially proposed by T. P. Hoar, was attempted. The experimental technique and the preliminary results are reported.

INTRODUCTION

The present paper describes current research in our laboratory. Emphasis was put on the electrochemical behavior of metals as related to pitting and stress-corrosion cracking. In the particular case of Al-Cu alloys it was found that there is a good correlation between pitting of Al with intergranular corrosion and with scc of Al-Cu alloys.

The anodic behavior of yielding metals, usually applied to study scc, was found very useful in the study of the mechanism of pitting of Al. These same studies gave evidence of the way pitting could lead to scc.

Considering the importance of the anion concentration to the anodic behavior of metals, the determination of Potential/Concentration diagrams for various Metal/Aqueous solution systems was initiated. The first results obtained are reported.

Morphology of pitting in aluminum

The study of pitting morphology in Al is of particular interest because, on the one hand, not all the reports available in the literature seem to agree, and, on the other hand, because although it shows an electrochemical behavior similar to that of other pitting systems [1], the shape of the pits in Al is not the usual hemispherical electropolished one found in other systems. The confusion in the literature comes from the fact that while some authors reported tunnel-like pitting in Al [2, 3], others described the pitting in Al as hemispherically shaped [4]. On the other hand, while some authors [1, 4, 5] described pitting of Al in chloride solutions as a typical high-potential passivity breakdown, others [6, 7] associated pitting only with bright electropolished pits. According to the last authors crystallographic etching, as found in Al, should occur only below the Flade potential, as happens in the case of Fe-Cr alloys in sulphuric acid [8].

During the present work the morphology of the pitting of pure Al in Cl^- solutions, in NO_3^- solutions, and in mixtures with different anions was studied. Measurements were performed on Al 99.99 % specimens annealed for 2 h at 600°C and water quenched. The edges and the surface of the specimens were covered with a cured-epoxy resin, leaving an uncovered area of about 1 sq. cm. The specimens were electropolished in a $HClO_4$-acetic anhydride bath, and stored in a desiccator for a few days before the experiments. The solutions were prepared with analytical

grade reagents and were deaerated with purified N_2. The potential was controlled with a Tacussel PRT 20-2-X potentiostat. All the measurements were made at 25°C.

Pitting of Al is known to occur in solutions of NaCl [1, 4, 5, 9], KBr[1, 4, 5], KI [1, 4], $NaClO_4$ [1, 5] and $NaNO_3$ (1). During the present experiments it was found that the pitting of Al also occurred in 1M NaSCN at 1.2 V (nhe). The pitting potentials in the different solutions are compared in Fig. 1.

The pitting of Al in neutral deaerated NaCl solutions was found to develop clearly geometrical forms, Fig. 2. This type of behavior is similar to that reported by Edeleanu [2] in constant current experiments. Hemispherical pits, as those found by Kaesche [4] in pH 11 NaCl solutions were not found in neutral NaCl solutions. As reported below, hemispherical pits were found in pH 11.0 deaerated 4M NaCl solutions but, if the pits were allowed to propagate long enough, they developed crystallographic planes similar to those found in neutral NaCl solutions.

Apart from the geometrical shape mentioned above, very well developed crystallographic planes were observed inside the pits formed in neutral NaCl solutions, Fig. 3. According to Edeleanu [2] these crystallographic planes are the (100) planes. It was also observed, as previously reported by the same author, that the pits formed in neutral NaCl solutions propagated deep into the volume of the metal. Crystallographic pitting similar to that observed in NaCl solutions was found in pits produced by KBr, KI, $NaClO_4$ and NaSCN solutions.

The pits produced in $NaNO_3$ solutions, on the other hand, showed a completely different morphology. In deaerated 1M $NaNO_3$ solutions the pitting of pure Al occurred at potentials higher than 1.7 V (nhe). In those solutions the pits were found to be of a circular shape and they were frequently covered by a poorly adherent corrosion product. This corrosion product, amorphous to the electron diffraction, is supposed to be Al_2O_3, n H_2O. Removing the corrosion product, hemispherical electropolished pits could be observed, Fig. 4. Inspected with the Scanning Electron Microscope (S.E.M.), the bottom of the pits showed the typical "dried mud" structure, Fig. 5.

With more diluted solutions, i.e. 0.1 M $NaNO_3$, the pits tended to lose their hemispherical shape, and flat surfaces developed inside the pits. By plastically deforming the pitted specimens and comparing the orientation of the flat surfaces in the pits with the slip lines produced by deformation those surfaces appeared to correspond to (111) planes, Fig. 6.

Measurements made in mixtures of NaCl plus $NaNO_3$ solutions showed that the pitting potentials and the morphology of the pits were strongly affected by the composition of the solution.

determined on wires previously deformed to 5 % elongation in air. This deformation was applied to the specimens to compensate any effect that the strain might have on the polarization curve.

The results in Fig. 18 identify the "critical potential" observed during yielding with the pitting potential of the static metal. Below the pitting potential the maximum c.d. observed is function of the strain rate and it is not affected by the electrode potential. The higher the strain rate the higher the c.d. reached during the experiment. Above the pitting potential the c.d. during straining is higher than that in the static metal and a higher pitting density is observed.

The results in Fig. 18 can be interpreted as follows. Before yielding the Al carries an oxide film of the order of 30 Å (18). During yielding slip steps are formed on the surface of the metal. According to Thomas and Nutting (20) the slip lines observed on Al are composed by several steps of the order of 600 Å each, Fig. 19. The number of steps per line increases with the deformation of the metal. The aluminum oxide film being very fragile (21) the formation of each step should be expected to expose to the solution an oxide-free metal surface. Since the rest of the surface of the metal is not disturbed, all the current increase observed during yielding below the pitting potential should concentrate on those steps. The value of the maximum c.d. observed during straining Al in neutral NaCl solutions, below the pitting potential, is similar to the one reported by bubar and Vermilyea (21) for straining Al in Ammonium Borate solutions. In the experiments of Bubar and Vermilyea the only possible anodic reaction on the yielding Al was the refilming of the metal. The similarity in the c.d. values and the fact that no pitting is observed on specimens yielded below the pitting potential in a NaCl solution lead to the conclusion that if oxide-free Al is exposed to a neutral deaerated NaCl solution, below the pitting potential, the only anodic reaction occurring on the metal will be film formation.

The effect of strain rate on the c.d. at potentials below the pitting potential, is explained by the analysis made by Staehle and Murata (22) on the effect of yielding over passive metals. It is based on the idea that if a constant strain rate is applied to a metal, the number of slip steps produced per unit of time will be constant. If repassivation is the only anodic reaction, each step will become inactive after a while. During yielding a stationary state will be reached when the number of new steps produced at any time is equal to the number of steps repassivated during the same time. The c.d. measured under those conditions should be constant. Under conditions of constant repassivation rate, in the stationary state, the number of steps being repassivated will be proportional to the strain rate. The higher the strain rate the higher the stationary c.d.

At potentials higher than the pitting potential the c.d. for Al in NaCl solutions is much higher for the yielding metal than for the static metal. As mentioned above the pitting density is also much higher in the yielding metal than in the static metal. This indicates that the rupture of the oxide film facilitates the nucleation of pits by

increasing the number of nucleation sites.

Yielding in 1M $NaNO_3$ solutions and in 4M pH 11.0 NaCl solutions

Straining 99.999 % Al in neutral 1M $NaNO_3$ solutions at potentials below the pitting potential gave results similar to those found in neutral NaCl solutions. The pitting potential in this solution was 1.7 V (nhe). Yielding experiments below this potential showed that the c.d. increased quickly up to a stationary value, Fig. 20. Interruption of straining, at those potentials, was followed by a rapid current decay to the low initial c.d. value. Observation of the specimens with the light microscope or with the S.E.M. did not reveal any pitting on the deformed specimens. By observation with the S.E.M. no difference between specimens strained in 1M $NaNO_3$ solutions, at potentials below the pitting potential, and specimens strained in air was observed, Fig. 21.

When straining the metal in $NaNO_3$ solutions at potentials higher than the pitting potential the c.d. never reached a constant value but kept increasing during all the experiment. Interruption of the straining, at potentials near the pitting potential, produced a small current decay. At higher potentials the current kept increasing even after interruption of straining.

During yielding at potentials higher than the pitting potential the c.d. was found to follow a law of the type:

$$J = a.t^b , \qquad [1]$$

where: J = current density,
t = time,
a, b = constants.

In a range of potentials of about 100 mV over the pitting potential, potentiostatic yielding of Al in a deaerated 1M $NaNO_3$ solution gave b = 2. A straight line is obtained when plotting the sq. root of the c.d. in function of time, Fig. 22. Light microscope observation of the yielded specimens showed the presence of lose white corrosion products over the slip bands. No pitting was observed on these specimens. The fine structure of the corroded slip bands could not be resolved with the S.E.M. Nevertheless it was observed that on specimens strained above the pitting potential the slip bands appeared heavily marked, Fig. 23, while it was difficult to observe them on specimens deformed below the pitting potential.

When the potentiostatic yielding of Al in 1M $NaNO_3$ solutions was done at potentials over the range mentioned above, b was higher than 2 and pitting nucleation is observed on the yielded specimens.

Potentiostatic measurements made on static Al in a 1M $NaNO_3$ solution, at potentials higher than the pitting potential, gave a value of b = 3. The cube root of the c.d. gave a straight line with time, Fig. 24. Under such conditions hemispherical pits were formed on the specimens.

Kaesche (4) reported that hemispherical pits are formed on Al in pH 11.0, deaerated, 4M NaCl solutions. By potentiostatic polarization of static Al this author found a value of b = 3, Fig. 25. During the present work, for polarization lengths similar to those reported by Kaesche, the formation of hemispherical pits was confirmed. Potentiostatic yielding experiments with Al in this solution gave b = 2, Fig. 26, for potentials higher than the pitting potential. The range of potentials where the behavior b = 2 was found, was much smaller than in $NaNO_3$ solutions, about 20 mV. But, as with $NaNO_3$ solutions, no pitting was observed on specimens yielded under conditions giving b = 2. The S.E.M. micrographs showed, as with nitrate solutions, that the slip bands in Al were heavily marked on specimens yielded above the pitting potential, while they were difficult to detect on specimens yielded below the pitting potential.

Discussion of the potentiostatic yielding experiments

The c.d./time curves found for potentiostatic yielding of Al in $NaNO_3$ solutions and in alkaline NaCl solutions, above the pitting potential, can be interpreted from the morphology of the pits.

Engell and Stolica (23) showed that the relation:

$$J = a.t^3 \qquad [2]$$

is obtained during pitting of metals, but the following conditions are necessary:

1 - The pits must grow in hemispherical shape,

2 - The c.d. inside the pits must be constant,

3 - The number of pits per unit area must increase in a linear function with time:

$$N = A.t \qquad [3]$$

where:

N = number of pits per unit area,
A = constant,
t = polarization time.

Engell and Stolica [23] showed that equation [2] is valid for the pitting of iron in sulphuric acid containing chloride ions. The same equation was found valid by Kaesche [4] for pitting growth in Al in alkaline NaCl solutions. The conditions established by Engell and Sotlica were fulfilled in pitting of Al in a $NaNO_3$ solution, where hemispherical pits were produced, and where the c.d. increased with time according to [2].

The potentiostatic c.d./time curves for yielding Al can be explained in a very similar manner. Following the arguments used by Engell and Stolica it results that to get a relation:

$$J = a.t^2 \qquad [4]$$

the following contidions should be fulfilled:

1'- Pitting must grow in semicylindrical shape, with the axis lying parallel to the surface of the metal.

2'- The c.d. inside the pits must be constant.

3'- The number of semicylindrical pits, per unit area, must increase as a linear function with time.

All these conditions are fulfilled for potentiostatic yielding Al in $NaNO_3$ solutions and in alkaline NaCl solutions. The condition 1' appears to be fulfilled because all the pitting is nucleated on the slip bands, and the semicylindrical pits appear as a natural modification of the hemispherical pits found on static metal. Condition 2' should be fulfilled on a yielding metal wherever condition 2 is fulfilled on a static metal. As for condition 3' it appears as a result of the experimental method, since as a constant strain rate is imposed to the wire, the number of steps formed per unit of time should be constant.

The potentiostatic yielding experiments so far described show that while under certain conditions the straining of the metal contributes to extend pitting, as with Al in neutral NaCl solutions, there are other conditions under which the straining of the metal produces nucleation of pitting only on slip lines.

Existence of a pitting potential in Al

The particular type of morphology of the pitting of Al in Cl^- solutions could lead to the belief that this is not a real case of pitting. Although this subject has already been discussed in a previous paper [1], it seems convenient to insist on

a few points.

Fig. 27 shows a typical polarization curve of Al in NaCl solution. It is observed that after a range of potentials at which the metal remains passive, there is a critical potential above which the current shows a very high increase. This curve was determined in steps of 10 mV, waiting at each potential until a constant current was attained. Since it could be argued that not enough time was allowed at each potential, and that the critical pitting potential could be much lower under other experimental conditions, a series of experiments was performed to study the effect of polarization time over the pitting potential. These experiments consisted in recording changes in the anodic c.d. for 5 h when specimens of Al were held at various constant potentials in 1M deaerated NaCl solutions, Fig. 28. When the potential was maintained at different values up to -0.53 V (nhe) the c.d. remained below 1 μA/sq. cm after 5 h and no pitting was observed. But with a potential only 10 mV higher than -0.53 V (nhe) the c.d increased by more than three orders of magnitude and pitting commenced. These experiments showed that if there is an induction time for the pitting of Al, a change in potential of 10 mV should decrease the induction time by at least four orders of magnitude. Therefore it can be concluded that pitting of Al is related to a critical potential which does not depend on an induction period.

Nevertheless Figs. 27 and 28 give by no means a complete description of pitting of Al. During the polarization curve measurement, there are other phenomena which cannot be ignored. Although a stationary c.d. is attained after a short potentiostatic polarization, there are flicks of current clearly detectable.

Fig. 29 shows the recording for a polarization curve for Al determined in 1M deaerated HCl solution. At low potentials no flicks were detectable. As the potential was increased the number of perturbations per unit of time increased, and finally at the pitting potential the concentration of those flicks was so high that it produced an increase in the total c.d. measured. In neutral NaCl solutions the perturbations observed were usually higher than those in acid solutions.

This behavior is not exclusive for Al. Similar oscillations were reported by Lotlikar and Davies [24] for high purity Zinc, and by Szklarska-Smialowska et al. [25] in stainless steels.

It was observed [26] that the current oscilations in Al in NaCl solutions were diminished or even suppressed if any surface-active agents were present in the solution.

Mechanism of pitting of Al

Although, as pointed out by Kolotyrkin [27] and by Hoar, Mears and Rothwell [7]

it is easy to understand why a pit propagates, it is not so easy to explain how it starts. Hoar, Mears and Rothwell suggested that at the pitting potential the aggressive anion, adsorbed on the oxide film surface, begins to penetrate the film under the influence of the electrostatic field across the film/solution interface when the field reaches a critical value corresponding to the breakdown potential.

The yielding experiments reported above show that the oxide film does not interfere with the anodic reaction occurring at the pitting potential. Exposing an oxide-free metal at a potential below the pitting potential, the only anodic reactions observed are oxide formation and repassivation. This indicates that the pitting potential is not related to an electrostatic field across the oxide/solution interface, and that pitting of Al is independent of any process of oxide film contamination. At, or near the pitting potential there must be some change in the metal/solution interface that conducts to a predominance of the dissolution reaction over the repassivation reaction. In those cases where information was available [28] it was found that the pitting potentials were very close to the zero charge potentials (z.c.p.), Table I. An oxide-free metal exposed to a solution at a potential below the z.c.p. will be predominantly faced with positive ions and water molecules. Under such conditions the reaction of the metal ions with the water molecules which gives an oxide film will predominate over the reaction of dissolution of the metal. Over the z.c.p. the oxide-free metal will be faced with an increasing number of negative ions. It is well known that the negative ions accelerate the anodic dissolution of the metals [29]. Under those conditions the process of metal dissolution will predominate over the process of metal passivation.

The z.c.p. would be the potential at which a pit could start, but a higher potential would be necessary to create the conditions that maintain an active pit. In the case of Al it is necessary to obtain a concentration of Cl^- ions high enough to maintain the corrosion products in solution inside the pit. If the electrolyte contains a high concentration of inactive ions, e.g. sulphate ions, see Fig. 11, the Cl^- ions will not reach the pit by transport and the pit will become inactive by occlusion with corrosion products. In this case oscilations in the current will be observed, but no stable pits will appear. If inside the pit we have $Al(NO_3)_3$ solution, which tends to decompose precipitating Al hydroxides [30], instead of having $AlCl_3$ solution which dissolves big amounts of Al hydroxides [31], the conditions for maintaining pitting will be complicated by the formation of solid products inside the pit. Higher pitting potentials should be expected to maintain the necessary transport of the aggresive nitrate ions through the amorphous alumina precipitate.

Those potentials for maintaining pitting, or pitting potentials, could be calculated from the transport data of the active species, the rates of the anodic and cathodic reactions, the rates of the chemical decomposition of the corrosion products, etc. An attempt to do such calculations was made by Kaesche [4] for pitting of Al in alkaline NaCl solutions.

Pitting and intergranular corrosion of Al-Cu alloys

In a recent paper [1] it was shown that by alloying Al with Cu the pitting potential of Al could be increased in more than 100 mV. In the same paper a mechanism for intergranular corrosion of aged Al-4 % Cu based on the difference in pitting potentials between the Cu-rich grain bodies and the Cu-depleted grain boundaries was proposed. Nevertheless the existence of a depleted region in aged Al-4 % Cu is open to discussion if the literature available on precipitation hardening (32) is taken into consideration. In view of this discrepancy further experiments with Al-Cu alloys were made.

The effect of Cu content on the pitting potential of Al-Cu in deaerated 1M NaCl solution was studied. Alloys of Al with 1; 2; 3; and 4 weight percent Cu were prepared with Al 99.99 % and Cu 99.999 %. The cast material was reduced by rolling to a thickness of 1 mm, and coupons of 10 x 30 mm were cut from the cold-rolled sheet. The coupons were solubilized for 2 h at 530°C and water quenched. A few specimens of Al-4 % Cu were used in solubilized condition, and the others were aged for different periods of time at 240°C. This temperature was chosen because it made it possible to obtain overaged material in a reasonable aging time. For the polarization measurements an electrical contact was made with a wire fastened to the specimen through a hole in it. The electrical contact wire, the edges of the specimen, and one of its faces were covered with an epoxy resin, leaving exposed a surface of about 1 sq. cm. Before the polarization measurements the specimens were electropolished in a 10 % HClO4 - Butilcellosolve mixture. Part of the aged specimens were used for hardness measurements. These specimens were electropolished as mentioned above, and the hardness was measured with a Durimet (Leitz, Wetzlar) microdurometer, with a load of 1000 g.

The pitting potentials were measured at 25°C in a deaerated 1M NaCl solution, by a galvanostatic method. A constant current of the order of 1 mA/sq. cm. was applied to the specimens and the potential changes were recorded. After a short polarization time the potential reached a stationary value, and the pitting potential was measured after 3 h of polarization. In each case the pitting potential value was confirmed by increasing the polarization current and checking whether the same stationary potential was obtained. The pitting potentials reported, Fig. 30, are the mean values measured on at least 5 different specimens. The scattering in the pitting potentials was lower than $\pm$ 10 mV. It was observed that by alloying Al with Cu a rapid increase in the pitting potential occurred for the first 1 % of Cu, and for higher Cu concentrations a linear relation was found between pitting potential and Cu content.

It is known that during the aging of Al-Cu a sequence of complex transformations occur in the matrix of the alloy. Al-4 % Cu was used to study the effect of aging on the pitting potential. The pitting potentials of the aged alloy were measured by the galvanostatic method. It was observed, Fig. 31, that the pitting potential of the alloy was very sensitive to the heat treatment. As previously mentioned [1] the

pitting potential of the overaged alloy was more than 100 mV lower than that of the solubilized alloy. The hardness measurements are included in Fig. 31 for reference. The hardness curve obtained in the present experiments is coincident with the measurements reported by Hardy (33) for en Al-4.0 % Cu alloy aged at 240°C.

It was found that the pitting potential decreased as soon as the hardness of the alloy started to increase. At 240°C the only precipitate formed in Al-4 % Cu is $\underline{\theta}'$ Phase (34). Beck showed (35) that in Al-4 % Cu aged at 240°C the $\underline{\theta}'$ phase precipitate was surrounded by a copper depleted region. This author could not detect by de oxide replica method any precipitate after the aging time required for peak hardness. Nevertheless Beck found that at peak hardness the copper content of the matrix was only 0.5 %. From Fig. 30 we found that the pitting potential for an alloy of Al-0.5 % Cu would be about -0.46 V (nhe). On the other hand, at peak hardness, Fig. 31, the pitting potential found was -0.48 V (nhe). This showed a good agreement with the matrix concentration value reported by Beck.

Pitting in aged Al-4 % Cu was distributed along very well defined lines, Fig. 32. The orientation of these lines changed from grain to grain, showing that they were related with the crystallographic orientation of the grains. By X-Rays diffraction it was found that these lines coincided with traces of planes (100). As it is known (32), the $\underline{\theta}'$ phase precipitates along the planes (100).

The present results could be used to explain the variation of pitting potential with aging of the alloy found in Fig. 31. It is observed that in the transition between solubilized alloy and over-aged alloy the pits are distributed along the (100) planes which are the matrix habit planes for $\underline{\theta}'$ phase. As shown by Beck the $\underline{\theta}'$ phase is surrounded by a solute depleted zone. On the other hand the Cu concentration reported by Beck for the matrix at peak hardness is coincident with the values expected from Figs. 30 and 31. All these observations point to the conclusion that the changes in pitting potential found during aging of Al-4 % Cu were due to the solute depletion of the matrix produced by precipitation. To support this conclusion even further, pitting does not follow any more the $\underline{\theta}'$ phase precipitates but nucleates at random (1) when all the matrix has its minimum Cu content, as it is the case in the overaged condition.

At potentials below the pitting potentials reported in Fig. 31, no pitting of the type shown in Fig. 32 was detected any more. But there was still a range of potentials where intergranular corrosion occurred. A series of experiments was performed to determine the range of potentials and heat treatments that originated intergranular corrosion. The aged Al-4 % Cu specimens were exposed in the NaCl solution for about 20 h at constant potential. Afterwards the specimens were deformed by bending and observed under the microscope to detect any intergranular corrosion. As reported in a previous paper (1) intergranular corrosion in aged Al-Cu alloy occurs only above certain potential. Exposure to NaCl solution below that potential does not produce intergranular corrosion. Nor does intergranular

corrosion occur in solubilized or in overaged conditions. It is known that during aging precipitation starts at the grain boundaries and develops there at a higher rate than in the matrix of the alloys [36]. As shown by Galvele and De Micheli [1] in order to have intergranular corrosion a difference in the pitting potentials of the grain boundaries and the grain bodies is a necessary condition. In this way a hypothetical pitting potential curve can be drawn for the grain boundaries, Fig. 33, delimiting the regions for intergranular corrosion, passivity and pitting for Al-4 % Cu in 1M NaCl solution.

All the results obtained in the present work point to the fact that there is a solute depleted zone along the grain boundaries, and that during intergranular corrosion the attack localizes in that depleted zone. The confusion in the literature seems to arise from the way the theory of precipitation developed. At the time the idea of a solute depleted zone was applied to intergranular corrosion [37] the precipitate free zone along the grain boundaries was assimilated to a solute depleted zone [36, 38]. Later it was found that the precipitate free zone was not due to solute depletion, but to vacancy depletion [32]. This observation was extended by some authors to the process of intergranular corrosion [39] assuming that there was not any solute depleted zone in the grain boundaries. Nevertheless no information is available supporting the idea that a depletion of vacancies could affect the electrochemical behavior of a metal. It seems more reasonable to conclude, as shown by Kelly and Nicholson [32] for Al-4.4 at.% Ag, that the precipitate free zone and the solute depleted zone are different zones, the latter being the smaller of the two.

Anodic behavior during yielding of Al-Cu

The anodic behavior of solubilized Al-4 % Cu wires in deaerated 1M NaCl solutions during yielding was studied, Fig. 34. The yielding experiments were made at different constant potentials with an initial strain rate of 90 %/min. As with pure Al, it was observed that the current increase to a stationary value, and that the stationary current varied with the potential. Here again it was observed that the influence of the potential on the maximum c.d. was lower below the pitting potential than above it.

As with Al, it is supposed that below the pitting potential the current increase is due to repassivation, while above the pitting potential it is due to pitting. Comparing the values in Fig. 34 with those for pure Al, Fig. 14, it is found that in a range of more than 100 mV while Al shows intense pitting during yielding, Al-Cu only shows the current increase due to repassivation. This range of potentials corresponds to the difference in the pitting potentials of both materials. Yielding both metals at an intermediate potential, Fig. 35, it is observed that the current increase for Al is almost three orders of magnitude higher than that for Al-Cu.

Yielding experiments were also performed with wires of aged Al-4 % Cu, Fig. 36. The deformation of the aged material is not homogeneous. Most of the deformation occurs in the precipitate-free zone along the grain boundaries, as shown with electron microscopy studies by Thomas and Nutting [38]. As shown above, that precipitate-free zone is composed of a large vacancy-depleted zone and a much smaller solute-depleted zone. The electrochemical behavior or the vacancy-depleted zone can be assimilated to the behavior or the solubilized Al-4 % Cu, while the behavior of the solute-depleted zone will be very similar to pure Al. From the experiments described above the anodic behavior of aged Al-4 % Cu during yielding in 1M NaCl solution can be predicted. It is evident from Fig. 35, that yielding, at constant potential, will not give an homogeneous distribution of attack in the soft precipitate-free zone. If the aged material is deformed at a potential below the pitting potential of the solute-depleted zone the only reaction on the metal surface will be repassivation of the metal. Above the pitting potential of the solute-depleted zone the deformation will generate intense corrosion of this zone, while the vacancy-depleted region will still show a process of repassivation. This localized corrosion will generate intergranular fisures propagating by mechanically intensified pitting of a narrow front along the grain boundaries, i.e. stress-corrosion cracking. Such behavior can be checked by measuring the elongation of aged Al-4 % Cu wires in 1M deaerated NaCl solution at constant potential, Fig. 37. It is found that if the potential is increased above the pitting potential of the solute-depleted zone there is a very high decrease in the ductility of the metal. On the other hand, if the metal is yielded at a potential below the pitting potential the elongations found are the same as obtained in air. The pitting potential of the solute-depleted zone is estimated from the measurements of solute depletion published by Beck [35], and the pitting potentials for different compositions of Al-Cu alloys given in Fig. 30. In all the yielding experiments of aged Al-4 % Cu, even in air, the fracture of the wires appeared to be intergranular. The oscilation of current observed during straining at low potential, Fig. 36, are attributed to the exposure of big oxide-free metal areas produced by mechanical tearing along the grain boundaries. At higher potentials the mechanical tearing is quickly overtaken by anodic dissolution along the grain boundaries. With a sufficiently low strain rate all fissure propagation would be due to anodic dissolution.

Scc of Al-Cu alloys

Mears, Brown and Dix [37] suggested that scc occurs along localized paths. The function of stress would be to open the crevices produced by corrosion. In the particular case of Al-Cu the localized path is the solute-depleted zone along the grain boundaries. According to the authors the corrosion of this zone would be due to a difference in potentials between the grain boundaries and the grain bodies. Logan [40], on the other hand, proposed a film-rupture mechanism by

which scc propagates due to rupture of the protective film and electrochemical dissolution of the unprotected metal. For scc of Al-Cu Colner and Francis [41] proposed a combination of both mechanisms. According to these authors the deformation localized along the grain boundaries will rupture the protective oxide film, fresh metal being thus exposed. There will be a constant tendency to refilm this naked metal. If the strain rate is slow the metal will have time to repassivate, but with a high strain rate the refilming will not be completed and the crack will propagate.

The results of the present work show that Logan's mechanism does not apply to Al and Al-Cu alloys. The plastic deformation could rupture the oxide film, but at potentials lower than the pitting potential the metal will repassivate as shown in Fig. 18. The strain rate is not important either, since a high strain rate will increase the number of slip steps undergoing repassivation, but will not change the type of anodic reaction.

The mechanism proposed by Mears, Brown and Dix is quite in agreement with the results of the present work. Nevertheless a few modifications should be made. As shown by Galvele and De Micheli [1] the existence of a depleted zone is a necessary but not a sufficient condition to produce localized corrosion. The presence in the media of anions capable of breaking the passivity of the alloy is also necessary. And the metal must be at a potential higher than the pitting potential of the depleted zone; otherwise the alloy will remain passive.

As for the effect of heat treatment on scc susceptibility, when aging over peak hardness, Fig. 31 the pitting potential of the grain bodies decreases very quickly. When the pitting potential of the grains is equal to the pitting potential of the boundaries corrosion will not concentrate any more on the grain boundaries, but it will spread all over the metal surface. Under such conditions the metal will not be susceptible to scc.

Stress, in the particular case of scc of Al-Cu alloys in neutral NaCl solutions, will open the fissures and accelerate the anodic process at the pitting potential.

Scc of other Al alloys

Since many age-hardenable Al alloys are susceptible to intergranular stress corrosion cracking, it would be interesting to see if the mechanism proposed for Al-Cu could be also extended to other Al alloys. Table II shows the pitting potentials in deaerated NaCl solutions for the phases present in aged Al-Cu alloys measured by Galvele and De Micheli [1], and for Al-Mg, and Al-Mg-Si, measured by Batrakov (42). In Al-Cu alloy the stresses will deform the soft zone along the grain boundaries,

where the depleted zone is present. If the potential is higher than the pitting potential of the depleted zone, corrosion will concentrate along the grain boundaries producing fissures, and the alloy will stress-corrode. In the Al-Mg alloy the solute depleted zone has the highest pitting potential, and the other two phases will corrode first. The lowest pitting potential corresponds to the hard intermetallic phase. In this alloy the only possible scc mechanism would be one of electrochemical dissolution of the intermetallic phase and simultaneous rupture of the Al rich zone by mechanical tearing. A mechanism like this is precisely what was proposed by Beck and Sperry [43] for scc of Al-Mg. Similarly for Al-Mg-Si scc will occur only by dissolution of the intermetallic phase. And as it is known, this alloy is susceptible to scc only under certain heat treatments where a continuous layer of the Mg_2Si is formed along the grain boundaries.

The comparison of these three Al alloys shows the complexity of the scc processes. The observations made on the mechanism of scc of one alloy allow no extrapolation to other alloys without a careful study.

Relation between pitting and scc

The relation found between pitting and stress corrosion cracking of Al-Cu alloys raises the question of how frequently both processes are related.

There are cases of stress corrosion where a good correlation between the conditions for pitting and those for scc is found. One example of this is the scc of Ti alloys in methanol plus HCl solutions [44]. In other cases, on the other hand, the literature is confusing as in the case of scc of stainless steels in $MgCl_2$. Staehle et al [45] found that the corrosion potential for stainless steel in boiling $MgCl_2$ corresponds to a passivity breakdown. Smialowski and Rychik on the other hand, found that the time to failure reached a maximum at that critical potential, Fig. 38. This Fig. was redrawn from the results of both papers [45, 46]. These results indicate that to get scc of stainless steel in $MgCl_2$ it is necessary to reach the conditions for pitting. Nevertheless Uhlig and Cook [47] discard any relaction between pitting and scc of stainless steel in $MgCl_2$, and Graf and Springe [48] consider that pitting and scc are related but competing processes;when one process occurs the other cannot occur.

In spite of these affirmations most of the results published point to the conclusion that in both cases the same anodic process is taking place. It is found that Ni increases the critical potential for scc [49] and also the critical potential for pitting [50]. Nitrates inhibit scc of stainless steels [47] but they also inhibit pitting [51]. Molibdenum seems to be an exception, since it is deleterious for stainless steel in boiling $MgCl_2$ [45] but inhibits pitting at room temperature [50]. Nevertheless Streicher [52] found that Mo is deleterious even for pitting at temper-

atures higher than 50°C.

The yielding experiments with Al showed that depending on the experimental conditions it is possible to nucleate pitting on the slip lines or to have it all over the metal. In $NaNO_3$ and alkaline 4M NaCl, when the potential is slightly higher than the pitting potential, pitting nucleates on the slip lines, but at higher potentials generalized pitting is observed. This could explain the competing behavior of pitting and scc found by Graf and Springe [48]. There should be a range of potentials where pitting nucleates at slip lines, giving the conditions for initiation of scc, while above these potentials pitting generalizes. According to this the mechanism of initiation of scc proposed by Smith and Staehle [53] should be modified stating that in the slip steps under the conditions for scc the repassivation process is replaced by a pitting process.

The way pitting could conduce to scc in different systems could be:

1) By dissolving a localized path, as in Al-Cu.

2) By localization on slip lines, as it seems to occur in stainless steels.

3) By production inside the metal of a local zone with an acid electrolyte, similar to that found in scc cracks [54, 55].

The criterion of correlation between pitting and scc has a practical implication. It gives the electrochemical conditions under which a metal should be tested for scc susceptibility. In our laboratory [56] Zircaloy-2 was found to be susceptible to scc in NaCl solutions if exposed at a potential near the pitting potential. It was also observed [57] that in NaCl solutions the AISI 4340 steel has a pitting potential equal to high purity iron, and that the 4340 steel has short time to fracture at the pitting potential while no fracture is observed at a potential silightly lower. In this case pitting acts perhaps, according to Fig. 39, by creation of a local acid solution, the conditions are set to initiate hydrogen embrittlement of the steel.

Potential/molar fraction diagrams

Hoar [6] in 1966 proposed the use of "potential/(anion/water)" diagrams for the display of experimental data available for passivity, anodic brightening, pitting, etc. Such diagrams have the advantage of showing in one single figure the effect of the electrode potential and the electrolyte composition on the anodic behavior of a metal. A few of these diagrams are being determined in our laboratory. The determination of the diagrams has not been completed yet and we are only reporting the experimental technique used and part of the results obtained. A discussion of the

results and their relation with previous work by other authors will be the subject of a separate paper [60]. It should be stressed that there is some difficulty in drawing such diagrams because while the definitions of good brightening, passivity, or etching are clear, there are wide transition zones where the denomination becomes subjective and exposed to discussion.

Experimental method. The determination of the diagrams was done in two steps. In a first series of experiments the polarization curve for each concentration was determined. The polarization curve was used to find out the potential ranges for the different form of anodic dissolution. A second series of experiments was performed to determine the morphology of the anodic attack. In these experiments the specimens were exposed at constant potential for different lengths of time. The exposure time varied from a couple of hours to various days. The exposure at constant potential lasted until the amount of metal equivalent to a penetration of 10 microns was dissolved. The potentiostatically corroded specimens were metallographically observed to find out the type of attack, and this information was used to draw the potential/concentrations diagrams.

Results: Cu-H_3PO_4-H_2O: Potentiostatic polarization curves were determined in deaerated 1M, 5M, 10M, and 14.6M H_3PO_4 solutions, Fig. 40. It was observed that the limiting current increased with the acid concentration. The potential-molar fraction diagram is very simple, Fig. 41, showing only active, etching, and brightening regions.

Ni-H_2SO_4-H_2O: The potentiostatic polarization curves, Fig. 42, are similar to those reported by Gilli et al. [61]. The Potential-concentration diagram, Fig. 43, is more complex, since there are regions of passivity, pseudo-passivity, and two different forms of pitting. In this case the morphology of the pits changed with the electrode potential.

Al-H_3PO_4-H_2O: Fig. 44 shows the potentiostatic polarization curves for this system. The diagram obtained, Fig. 45, is very simple, showing only etching, brightened pits and brightening.

CONCLUSIONS

From the results reported in this paper the following conclusions can be drawn:

1) Brightened hemispherical pits are not a general rule in pitting of metals.

2) Exposing bare aluminum to an "aggressive" solution, such as NaCl solutions or $NaNO_3$ solutions, does not lead to pitting, if the electrode potential of the metal is lower than the pitting potential.

3) Potentiostatic yielding experiments with Al show that the oxide film acts as an inert species in the pitting process.

4) Yielding of Al at the pitting potential can accelerate pitting nucleation, as in neutral NaCl solutions, or can lead to pitting nucleation on slip steps, as in $NaNO_3$ solutions and in alkaline NaCl solutions.

5) It is suggested that the experimental pitting potential is the potential for maintaining pitting. The potentiostatic yielding experiments and the effect of surface-active agents on the current oscillations indicate that the initiation potential for pitting should be related with the zero charge potential of the metal.

6) In contradiction with recent literature on aging mechanisms of Al alloys, evidence is given of the existence of a solute depleted zone along the grain boundaries of aged Al-Cu alloys.

7) The pitting potential of Al-4 % Cu depends on the heat treatment, and shows an important drop when the alloy comes close to peak hardness.

8) Potentiostatic yielding experiments with Al-4 % Cu show that scc susceptibility of the alloy begins when the metal reaches the pitting potential of the depleted zone.

9) A mechanism of scc based on an anodic dissolution of a depleted zone is applicable to Al-Cu alloys, but cannot be extended to other Al alloys, such as Al-Mg or Al-Mg-Si.

10) There is good correlation between pitting and scc. Three mechanisms are suggested by which pitting could lead to the initiation of scc.
   i) By dissolution of a localized path, scc occuring only at potentials higher than the pitting potential of such path.
   ii) By nucleation of pitting on slip steps during mechanical deformacion of the metal. Scc will occur in the range of potentials where pitting nucleates only on slip steps. As soon as pitting nucleation starts on

other parts of the metal surface the susceptibility to scc disappears.

iii) By producing a heterogeneity in the electrolyte in contact with the metal. In the cases of hydrogen embrittlement, by creating a zone with an acidic solution capable of hydrogen evolution.

11) The criterion of pitting related with scc leads to a practical method for determination of the electrochemical conditions which conduct to scc susceptibility of an alloy.

ACKNOWLEDGEMENTS

We wish to thank Mr. F. Pedraza for excellent technical assitance during the potentiostatic yielding experiments.

We thank the Programa Multinacional de Metalurgia (Programa Regional de Desarrollo Científico y Técnico-O.A.S.) and the Consejo Nacional de Investigaciones Científicas y Técnicas of Argentina for financial support.

TABLE I

ZERO CHARGE POTENTIALS AND PITTING POTENTIALS (E_p)

METAL	z.c.p. ($V_{(nhe)}$) (28)	$E_p(V_{(nhe)})$	ELECTROLYTE	REF.
Al	-0.52 (KCl 0.01 M)	-0.40	NaCl 0.01 M	(1)
		-0.53	NaCl 1M	(1)
		-0.37	NaBr 1M	(1)
Fe	-0.33 - -0.40 (HCl 0.01 M)	-0.35	NaCl 0.5 M	(57)
Mg	-1.04 (*)	-1.2	NaBr 1M	(27)
		-1.45	NaCl 0.5 M	(27)
Ni	+0.29 (*)	+0.28	NaCl 0.1 M	(50)
Zn	-0.52 (*)	-0.78	NaCl 1M(pH 9.0)	(58)

(*) Values calculated with formula: $E_{z.c.p.} = W_e - 4.72$, from Ref. (28)

W_e values from (59).

TABLE II

PITTING POTENTIALS OF PHASES PRESENT IN AGED ALUMINUM ALLOYS

ALLOY	PHASE	$E_p(V_{(nhe)})$	REF.
Al-4%Cu	Al-Cu	-0.39	(1)
	Al_2Cu	-0.40	
	Al	-0.52	
Al-Mg	Al	-0.52	(42)
	Al-Mg	-0.60	
	Mg_2Al_3	-0.87	
Al-Mg-Si	Al-Mg-Si	-0.50	(42)
	Al	-0.52	
	Mg_2Si	-1.35	

REFERENCES

1) J. R. GALVELE and S. M. de DE MICHELI, Corrosion Sci. 10, 795 (1970)

2) C. EDELEANU, J. Inst. Metals, 89, 90 (1960)

3) F. J. BURGER, V. F. TULL and P. H. HARRIS, Bull. Inst. Metals, 3, 6 (1955-57)

4) H. KAESCHE, Z. phys. Chem., 34, 87 (1962)

5) H. BöHNI and H. H. UHLIG, J. electrochem. Soc., 116, 906 (1969)

6) T. P. HOAR, Corrosion Sci., 7, 341 (1967)

7) T. P. HOAR, D. C. MEARS and G. P. ROTHWELL, Corrosion Sci, 5, 279 (1965)

8) R. P. FRANKENTHAL, J. electrochem. Soc., 114, 542 (1967)

9) A. P. BOND, G. F. BOLLING, H. A. DOMIAN and H. BILONI, J. electrochem. Soc., 113, 773 (1966)

10) W. SCHWENK, Corrosion, 20, 129 (1964)

11) Z. SZKLARSKA-SMIALOWSKA and M. JANIK-CZACHOR, Corrosion Sci., 7, 65 (1967)

12) T. P. HOAR and J. C. SCULLY, J. electrochem. Soc., 111, 348 (1964)

13) J. C. SCULLY and T. P. HOAR, 2nd. International Congress on Metallic Corrosion, New York 1963. NACE, Houston 1966, p. 184

14) J. R. GALVELE, Anodic Behavior of Mild Steel During Yielding, Tesis, University of Cambridge, England 1966.

15) T. P. HOAR and J. R. GALVELE, Corrosion Sci., 10, 211 (1970)

16) J. J. PODESTA, G. P. ROTHWELL and T. P. HOAR, Corrosion Sci., 11, 241 (1971)

17) T. P. HOAR and R. W. JONES, Corrosion Sci., in press

18) M. J. PRYOR, Corrosion Sci., 11, 463 (1971)

19) J. A. RICHARDSON and G. C. WOOD, Corrosion Sci., 10, 313 (1970)

20) G. THOMAS and J. NUTTING, J. Inst. Metals, 85, 1 (1956-57)

21) S. F. BUBAR and D. A. VERMILYEA, J. electrochem. Soc., 114, 882 (1967)

22) R. W. STAEHLE and T. MURATA, The Ohio State University, Report No. COO-1319-71 (Q-19), June 1968

23) H. J. ENGELL and N. D. STOLICA, Z. physik, Chem. N. F., 20, 113 (1959)

24) M. M. LOTLIKAR and D. E. DAVIES, 3rd, International Congress on Metallic Corrosion, Moscow 1966, Proceedings of the Moscow 1969, Vol. I, p. 167

25) Z. SZKLARSKA-SMIALOWSKA and J. JANIK-CZACHOR, Br. Corros. J. 4, 138 (1969)

26) S. M. de DE MICHELI and J. R. GALVELE, in preparation

27) Ya . M. KOLOTYRKIN, Corrosion, 19, 261 t, (1963)

28) R. S. PERKINS and T. N. ANDERSEN, Modern Aspects of Electrochemistry, (Ed. J. O'M. Bockris and B. E. Conway) Plenum, New York 1969, Vol. 5, p. 203

29) Ya. M. KOLOTYRKIN, 3rd. International Congress on Metallic Corrosion, Moscow 1966, Proceedings of the Moscow 1969, Vol. I, p. 73

30) P. PASCAL, Nouveau Traité de Chimie Minérale, Masson et Cie. Ed. Paris 1961, Vol. VI, p. 635

31) T. HAGYARD and J. R. SANTHIAPILLAI, J. appl. Chem., 9, 323 (1959)

32) A. KELLY and R. B. NICHOLSON, Progress in Metal Physics. Vol. 10, p. 151, Pergamon Press 1963

33) H. K. HARDY, J. Inst. Metals, 79, 321 (1951)

34) J. M. SILCOCK, T. J. HEAL and H. K. HARDY, J. Inst. Metals, 82, 239 (1953-54)

35) A. F. BECK, J. Appl. Phys. 36, 2944 (1965)

36) H. K. HARDY and T. J. HEAL, Progress in Metal Physics, Vol. 5, p. 143, Pergamon Press, 1954

37) R. B. MEARS, R. H. BROWN and E. H. DIX (Jr.), ASTM-AIME, Symposium on Stress Corrosion Cracking of Metals, p. 323 (1945)

38) G. THOMAS and J. NUTTING, J. Inst. Metals, 86, 7 (1957-58)

39) F. J. KIEVITS and A. J. ZUITHOFF, J. Inst. Metals, 93, 517 (1964-65)

40) H. J. LOGAN, J. Research NBS, 48, 99 (1952)

41) W. H. COLNER and H. T. FRANCIS, J. electrochem, Soc. 105, 377 (1958)

42) V. P. BATRAKOV, 3rd. International Congress on Metallic Corrosion, Moscow 1966, Proceedings of the Moscow 1969, Vol. 1, p. 313

43) A. F. BECK and P. R. SPERRY, Fundamental Aspects of Stress Corrosion Cracking, Ohio 1967, Proceedings of Conference, NACE, Houston 1969, p. 513

44) M. LEVY and D. W. SEITZ (Jr.), Corrosion Sci., 9, 341 (1969)

45) R. W. STAEHLE, J. J. ROYUELA, T. L. RAREDON, E. SARRATE, C. R. MORIN and R. V. FARRAR, Corrosion, 26, 451 (1970)

46) M. SMIALOWSKI and M. RYCHCIK, Corrosion, 23, 218 (1967)

47) H. H. UHLIG and E. W. COOK, J. electrochem. Soc. 116, 173 (1969)

48) L. GRAF and G. SPRINGE, Fundamental Aspects of Stress Corrosion Cracking, Ohio 1967, Proceedings of Conference, NACE, Houston 1969, p. 335

49) H. H. LEE and H. H. UHLIG, J. electrochem. Soc., 117, 18 (1970)

50) J. HORVATH and H. H. UHLIG, J. electrochem. Soc. 115, 791 (1968)

51) H. P. LECKIE and H. H. UHLIG, J. electrochem. Soc., 113, 1262 (1966)

52) M. A. STREICHER, J. electrochem. Soc. 103, 375 (1956)

53) T. J. SMITH and R. W. STAEHLE, Corrosion, 23, 117 (1967)

54) B. F. BROWN, C. T. FUJII and E. P. DAHLEBERG, J. electrochem. Soc., 116, 218 (1969)

55) J. A. SMITH, M. H. PETERSON and B. F. BROWN, Corrosion, 26, 539 (1970)

56) G. CRAGNOLINO and J. R. GALVELE, in preparation

57) J. R. GALVELE and C. J. SEMINO, 2o. Simposio Latinoamericano de Corrosión, Río de Janeiro, 8-12 November 1971

58) G. ALVAREZ and J. R. GALVELE, in preparation

59) Handbook of Chemistry and Physics, 45th Edition, The Chemical Rubber Co. Ohio (1964) p. E43

60) I. L. ALANIS and J. R. GALVELE, in preparation

61) G. GILLI, P. BOREA, F. ZUCCHI and G. TRABANELLI, Corrosion Sci., 9, 673 (1969)

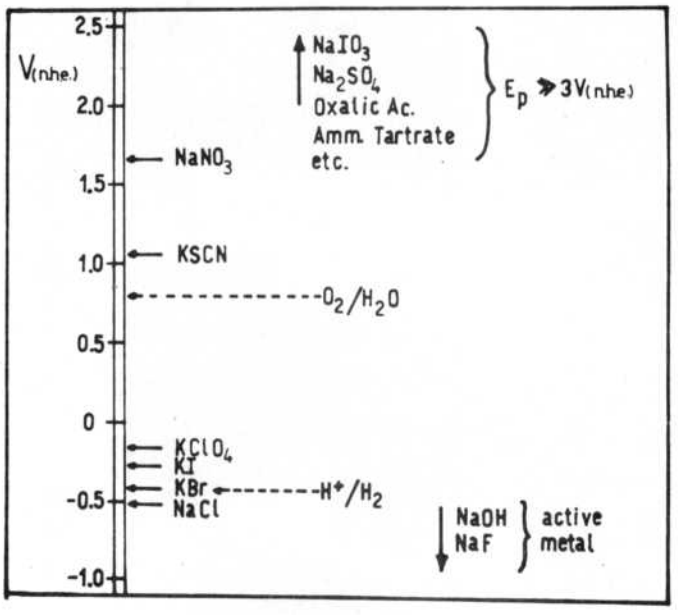

Fig.1- Comparison of the pitting potentials of Al in various electrolytes. The solutions were neutral and of 1M concentration, except for $KClO_4$ where 0.1M solution was used. The standard potentials for hydrogen evolution and for oxygen reduction in neutral solutions are included as a reference.

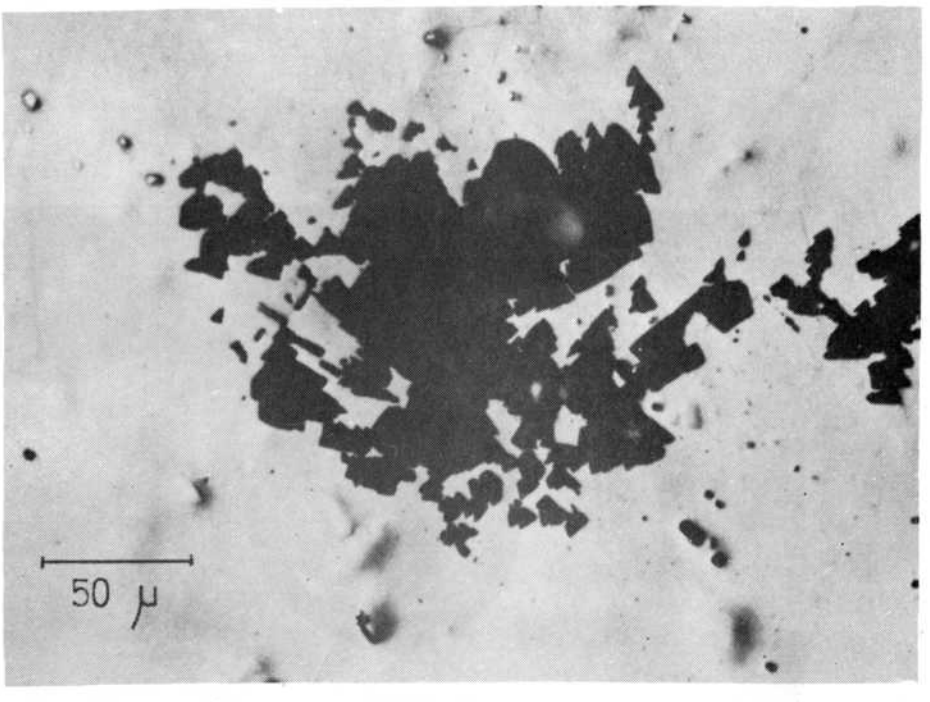

Fig.2- Pitting of aluminum in neutral deaerated 1M NaCl solution. The pits take different geometrical forms according to the orientation of the metal grains. In the figure predominance of triangular pits is observed.

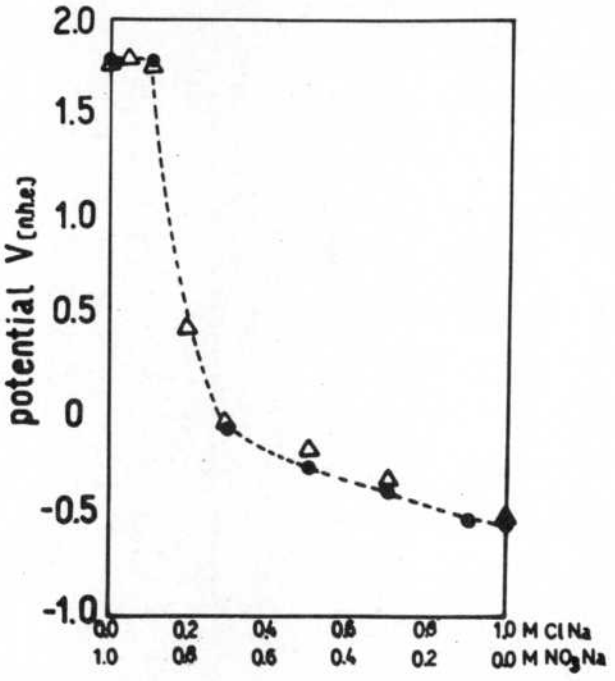

Fig.7- Pitting potentials of Al 99.99% in mixtures of NaCl plus $NaNO_3$ solutions. Δ:galvanostatic measurements; ●:potentiostatic measurements.

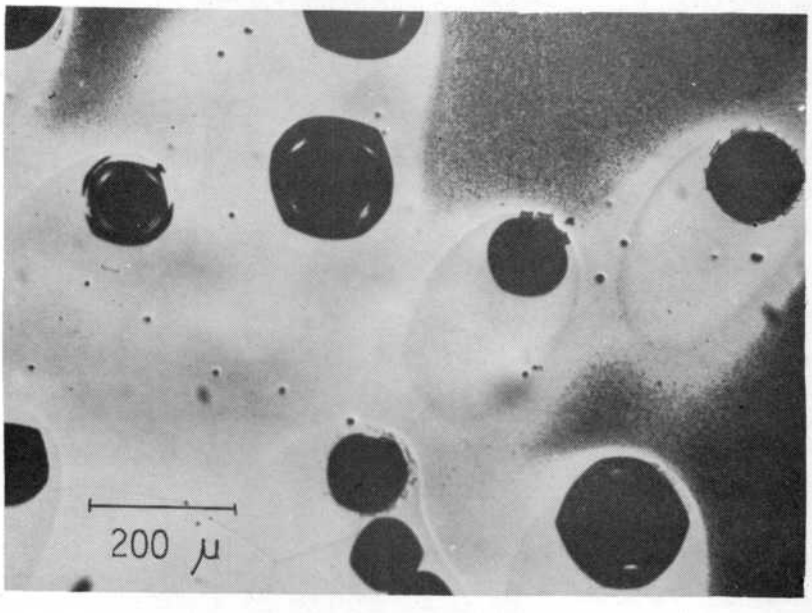

Fig.8- Pitting of Al in 1M $NaNO_3$ plus 0.05M NaCl solution. The morphology of the pits is the same as for pure $NaNO_3$ solutions.

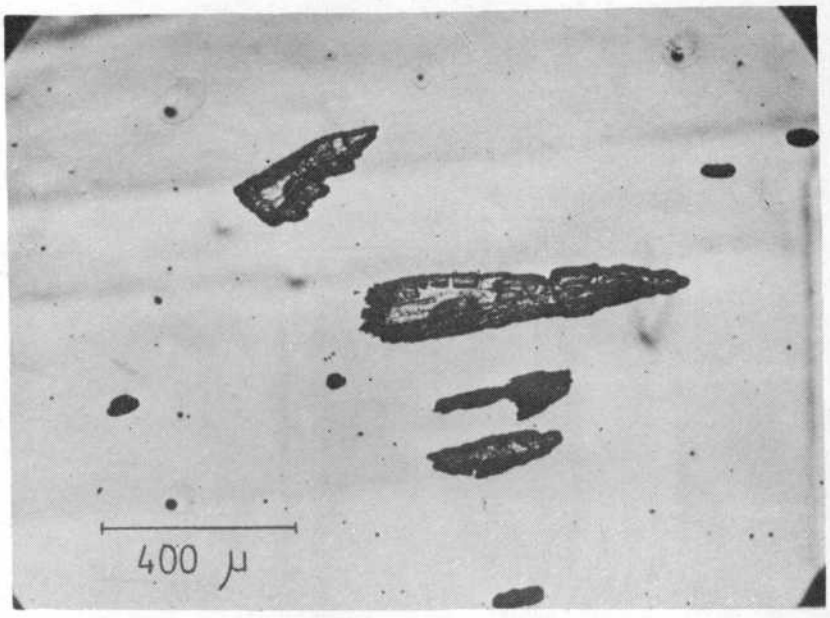

Fig.9- Pitting of Al in a 0.9M $NaNO_3$ plus 0.1M NaCl solution. The pitting potential is the same as for $NaNO_3$ solutions, but the pits are arrow-shaped and their interior is covered with a thick layer of corrosion products.

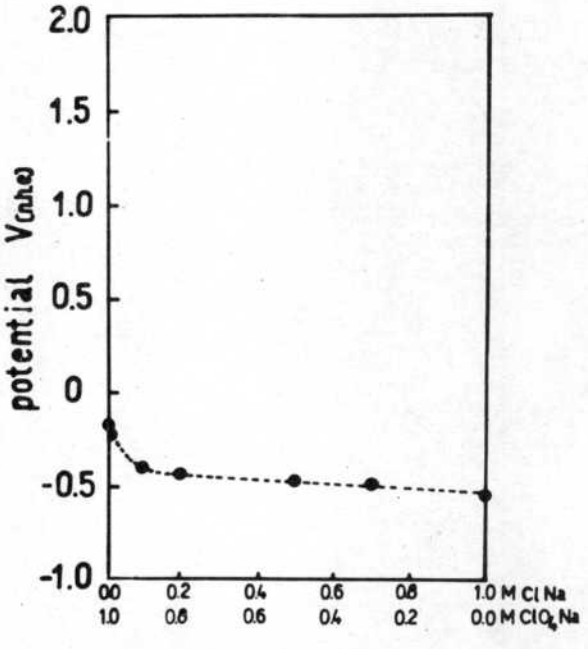

Fig.10- Pitting potentials of Al in neutral deaerated mixtures of NaCl plus $NaClO_4$ solutions at 25ºC.

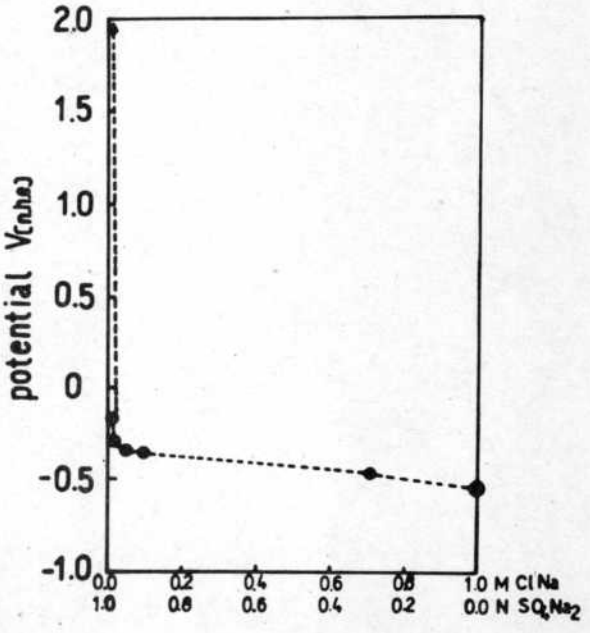

Fig.11- Pitting potentials of Al in neutral deaerated mixtures of NaCl plus Na_2SO_4 solutions at 25ºC.

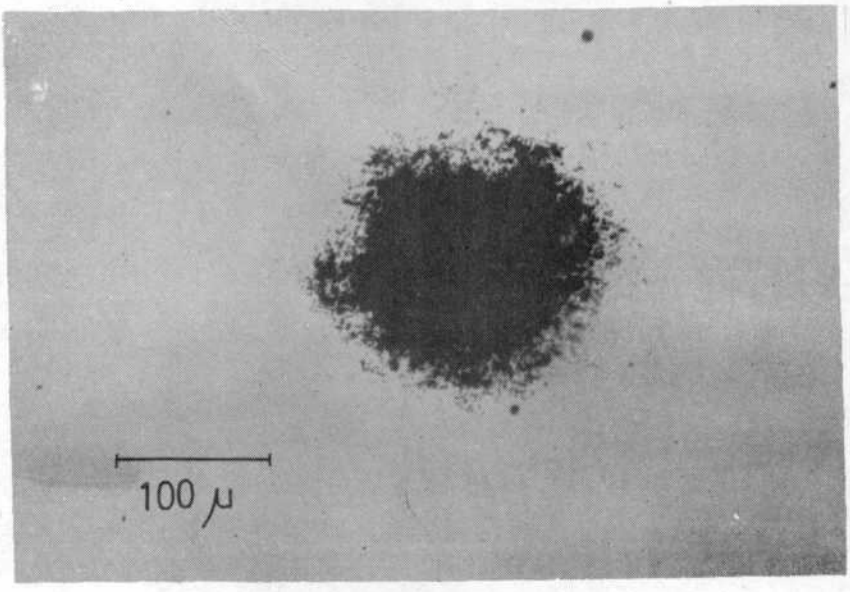

Fig.12- Pitting of Al in a neutral deaerated 0.5M Na_2SO_4 plus 0.01M NaCl solution at 25ºC. Pitting appears in the form of clusters of very small pits. The interior of the pits shows the same crystallographic etching found in pure NaCl solutions.

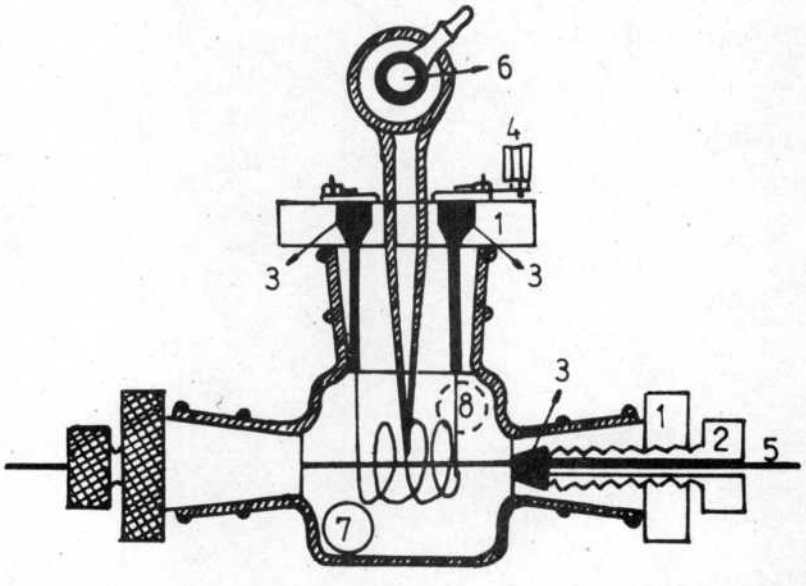

Fig.13- Cell for the study of the anodic behavior of yielding wires under constant potential. TOP VIEW: 1:Teflon conical plug; 2:Perspex screw; 3:Silicon rubber seals; 4:Platinum counter-electrode; 5:Specimen; 6:Reference electrode; 7:Deaerated solution inlet; 8:Solution outlet.

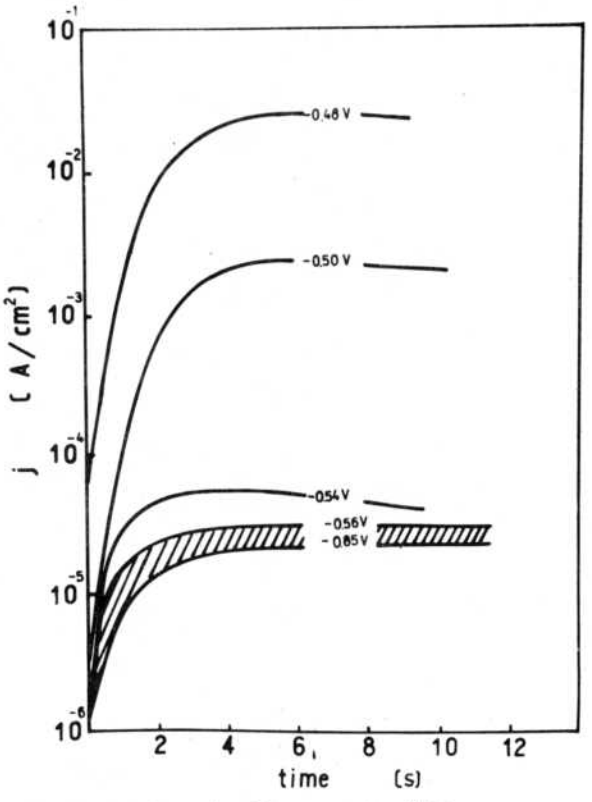

Fig.14- Potentiostatic c.d./time curves for Al 99.9% yielding in 1M deaerated NaCl solution at 25ºC. Initial strain rate: 90%/min.

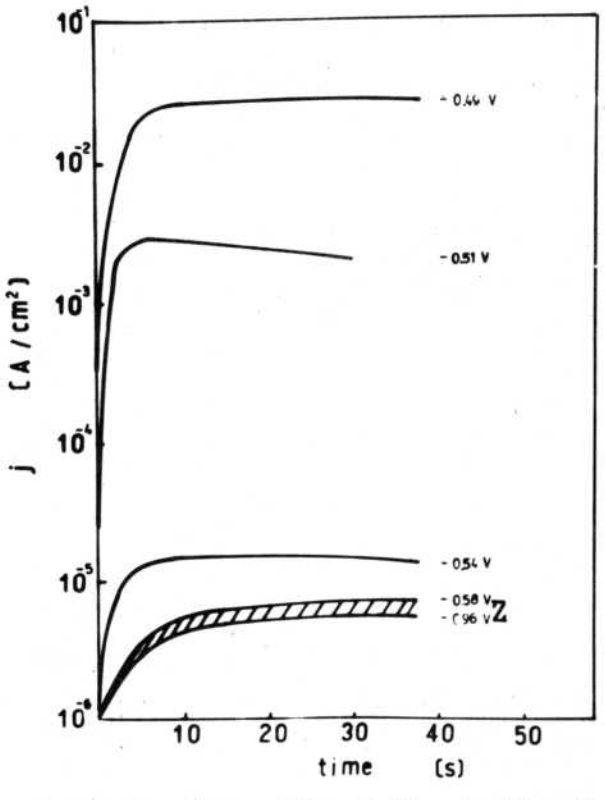

Fig.15- (Id. Fig.14). Initial strain rate: 21%/min.

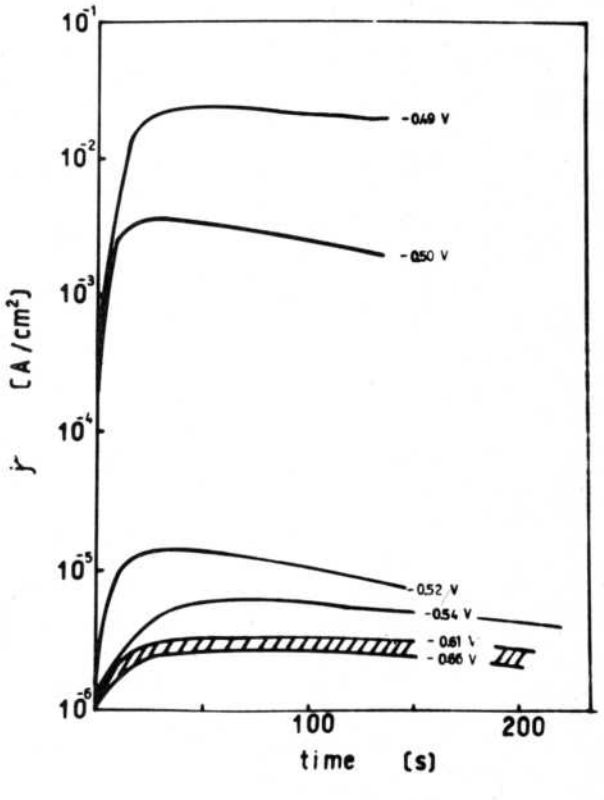

Fig.16- (Id. Fig.14). Initial strain rate: 5%/min.

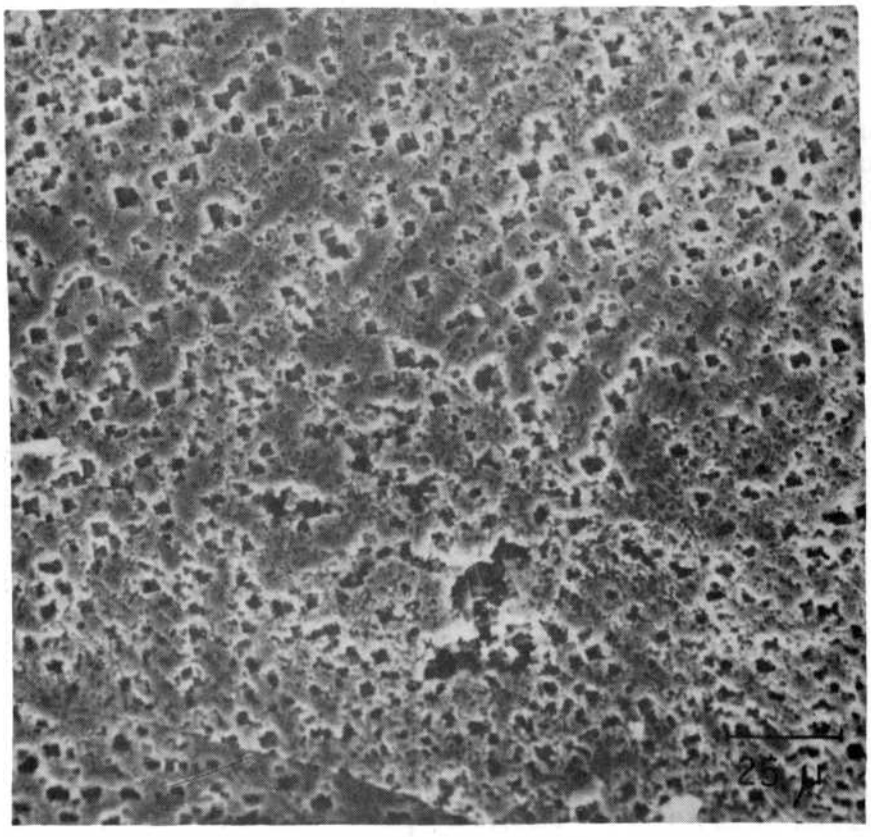

Fig.17- S.E.M. picture of Al 99.9% wire strained in 1M deaerated NaCl solution at -0.48 V(nhe). The surface of the wire appears heavily pitted.

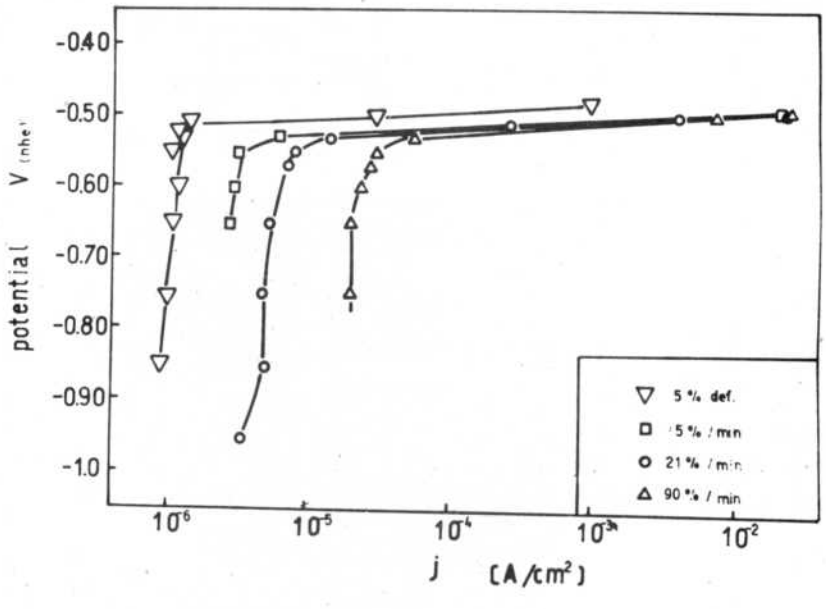

Fig.18- Stationary c.d.'s for Al yielding in deaerated 1M NaCl solution at 25ºC. Δ:90%/min; O:21%/min □:5%/min; ▽:Potentiostatic polarization curve for 5% deformed Al.

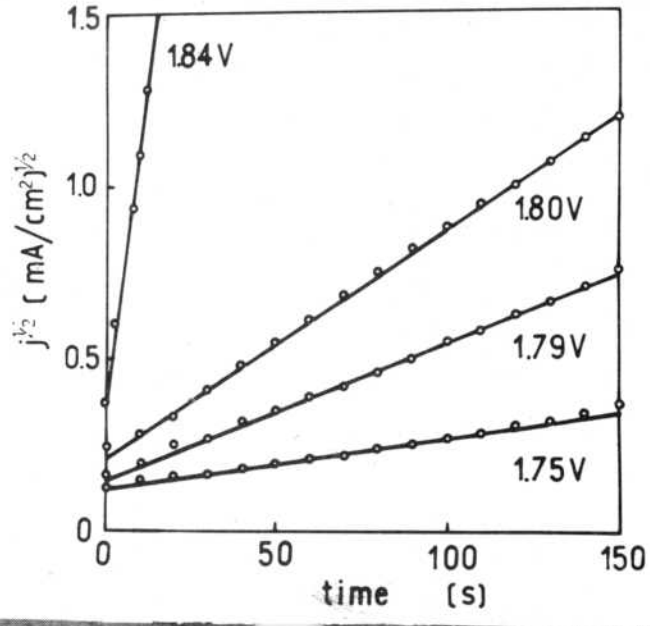

Fig.22- Potentiostatic yielding of Al 99.999% in 1M $NaNO_3$ solution at potentials higher than the pitting potential.

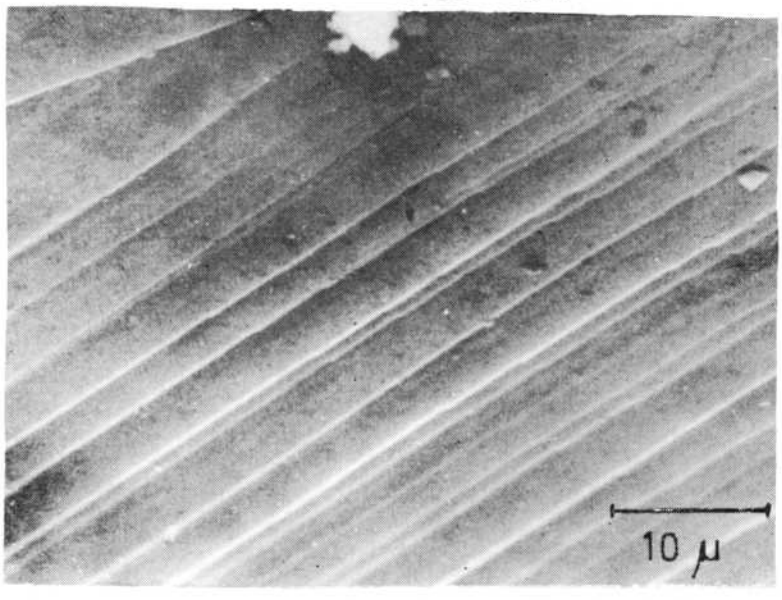

Fig.23- S.E.M. picture of Al 99.999% after yielding in 1M $NaNO_3$ solution at 1.8 V(nhe). Total elongation: 5%.

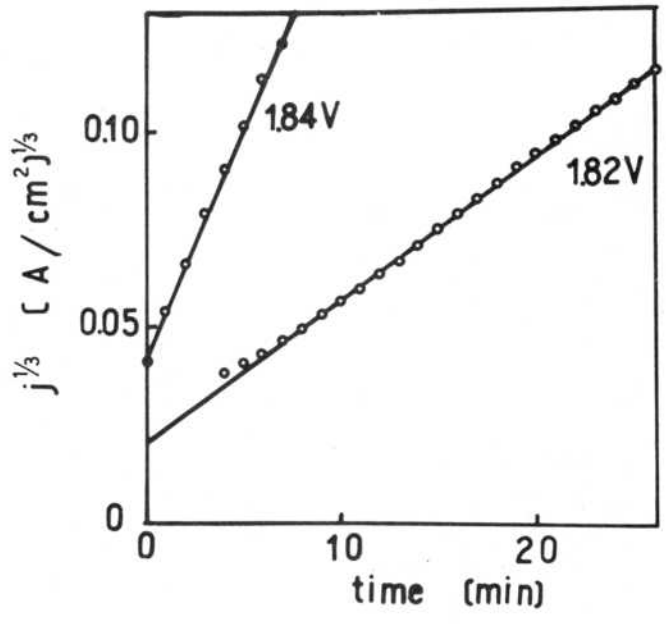

Fig.24- C.d./time curves for Al 99.999% polarized at constant potential in 1M $NaNO_3$ solution.

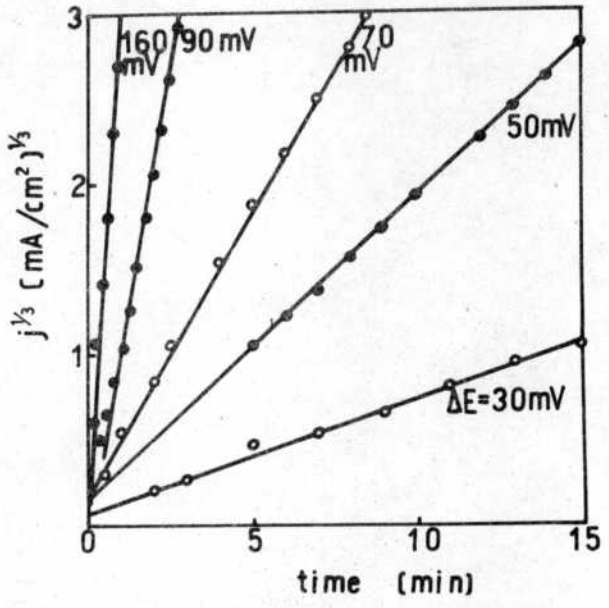

Fig.25- C.d./time curves for Al 99.99% polarized at constant potential in deaerated 4M NaCl solution, pH 11.0, according to Kaesche (4).

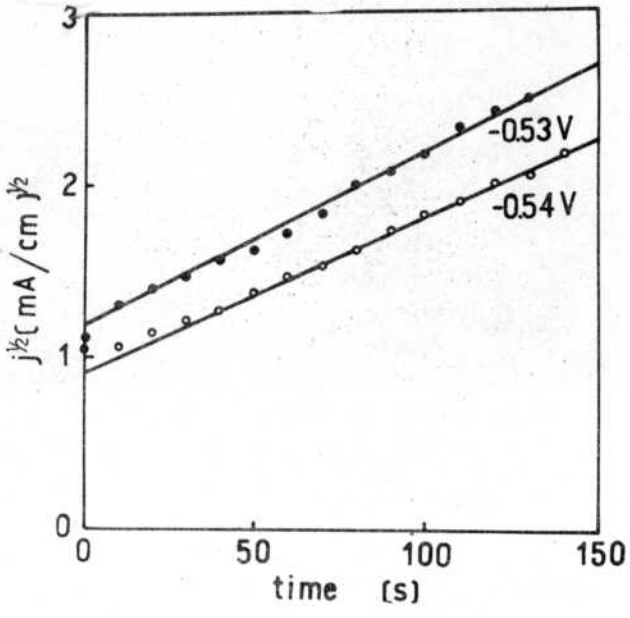

Fig.26- Potentiostatic yielding of Al 99.999% in deaerated 4M NaCl solution, pH 11.0.

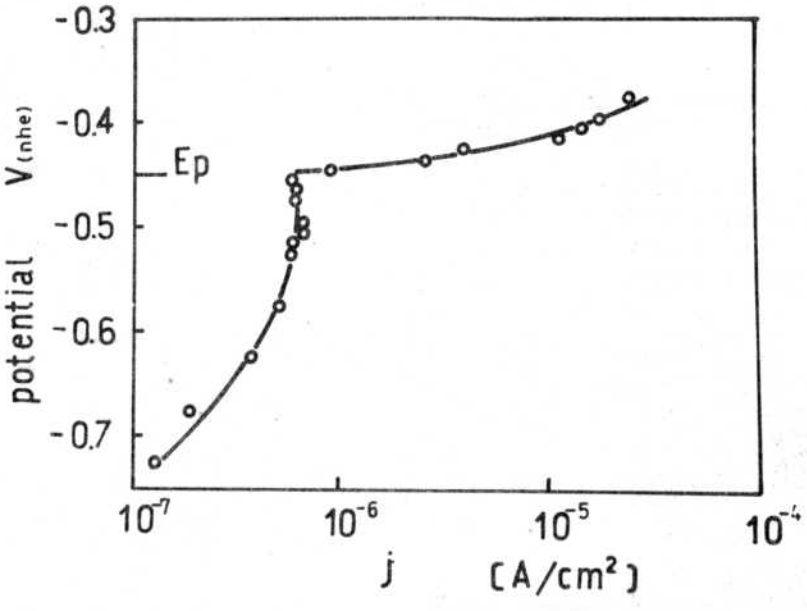

Fig.27- Anodic polarization curve of 99.99% Al in deaerated 0.1M NaCl solution. Ep: potential at which pitting starts.

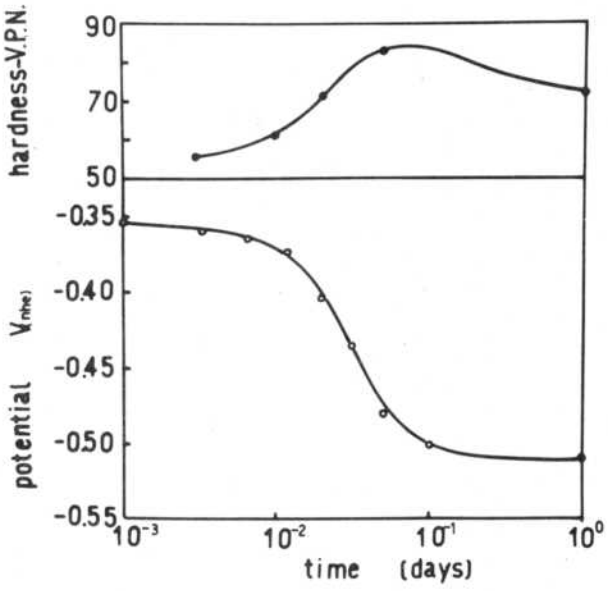

Fig.31- Effect of aging time on pitting potentials and hardness of Al-4%Cu aged at 240ºC. Deaerated 1M NaCl solution at 25ºC.

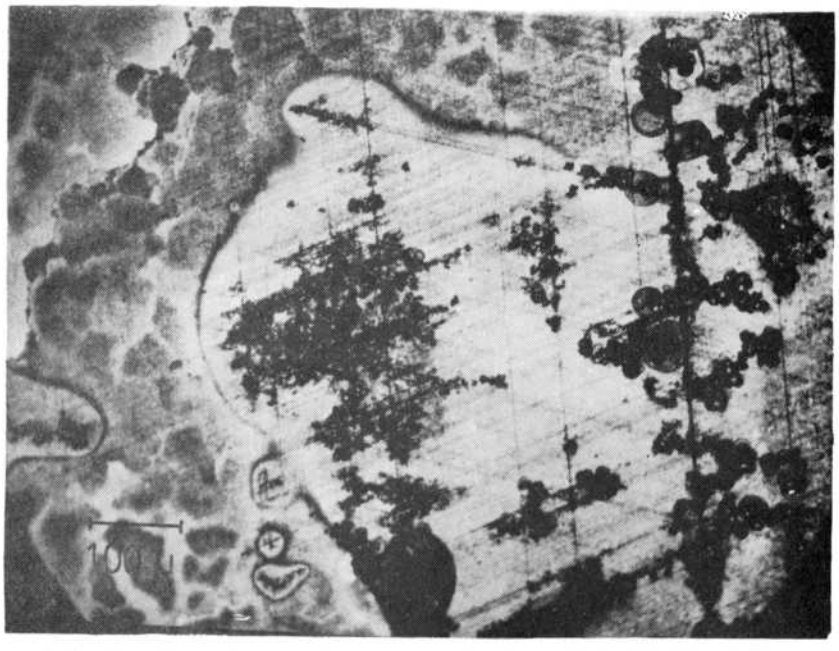

Fig.32- Pitting nucleated along (100) planes. Al-4%Cu aged 15 min at 240ºC. Deaerated 1M NaCl solution at 25ºC.

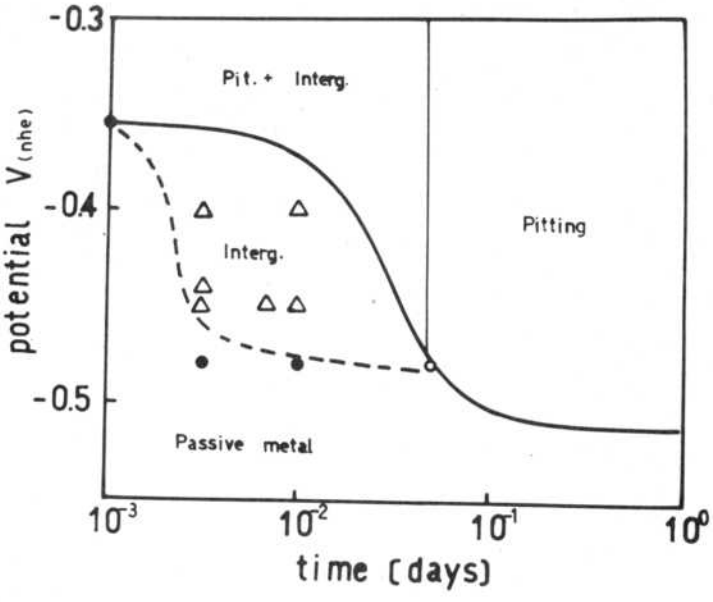

Fig.33- Effect of aging time on intergranular corrosion and pitting of Al-4%Cu aged at 240ºC. Deaerated 1M NaCl solution at 25ºC.

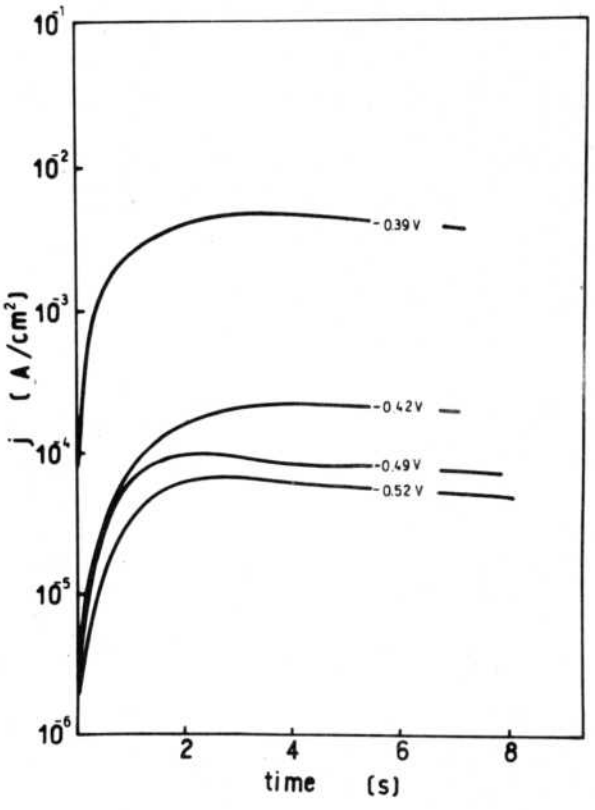

Fig.34- Potentiostatic c.d./time curves for yielding solubilized Al-4%Cu in 1M deaerated NaCl solution at 25ºC. Initial strain rate: 90%/min.

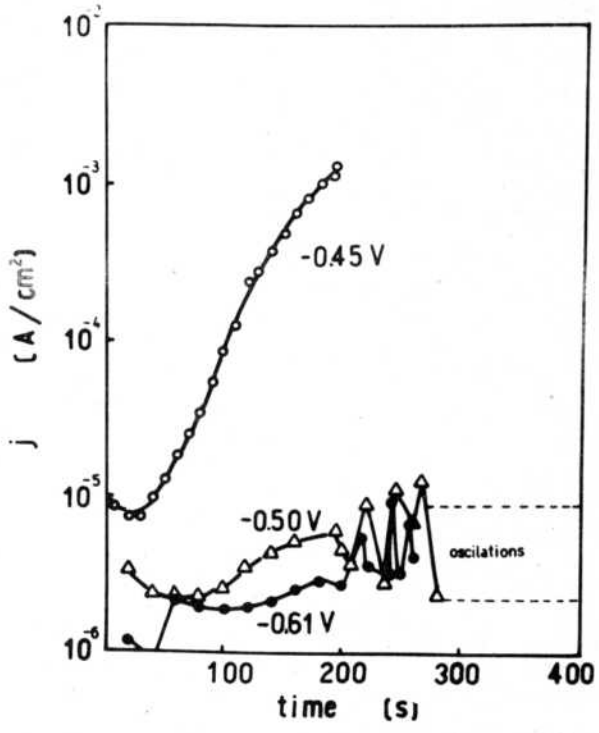

Fig.36- Potentiostatic c.d./time curves for yielding in 1M deaerated NaCl solution. Al-4%Cu aged 3h at 210ºC. Initial strain rate 1.6%/min.

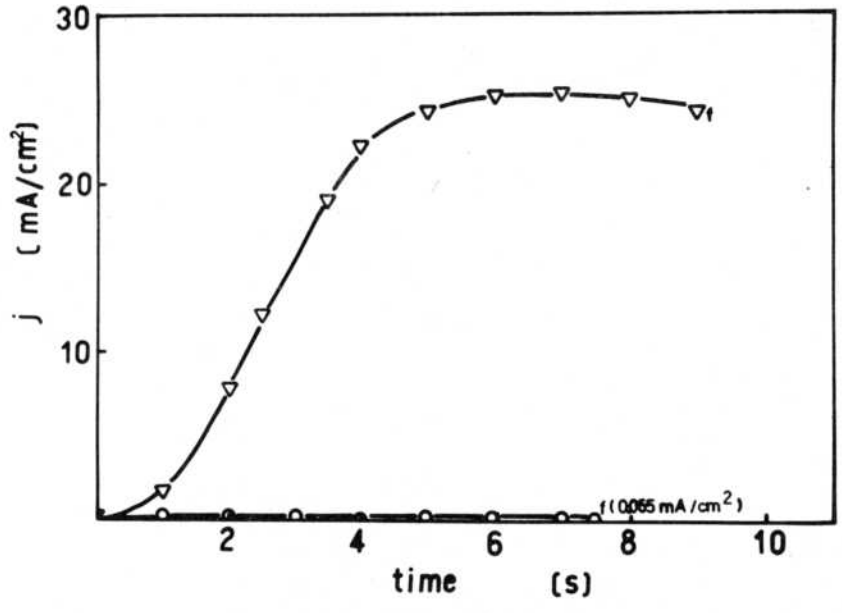

Fig.35- Potentiostatic c.d./time curves for yielding in 1M deaerated NaCl solution at -0.49V(nhe). Initial strain rate 90%/min. o:solubilized Al-4%Cu; ▽:Al99.99%.

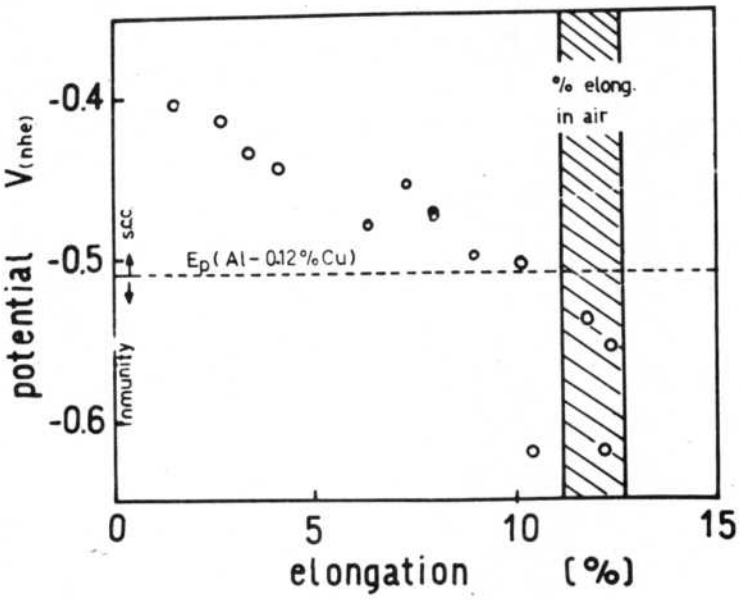

Fig.37- Effect of potential on ductility of aged Al-4%Cu during potentiostatic yielding in 1M deaerated NaCl solution. Aging: 3h at 210ºC. Initial strain rate: 1.6%/min.

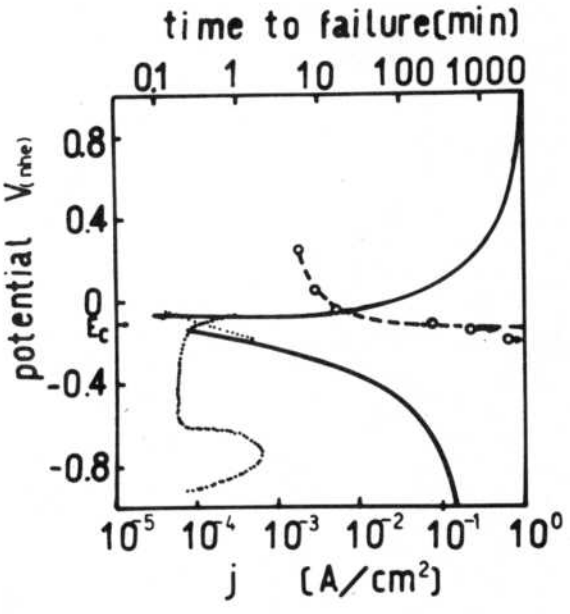

Fig.38- Potentiostatic polarization curve and effect of potential on ttf for type 302 steel in 35 w/o $MgCl_2$ solution at 125ºC; from Smialowski et al. (46). Dotted line: actual anodic curve from Staehle et al. (45).

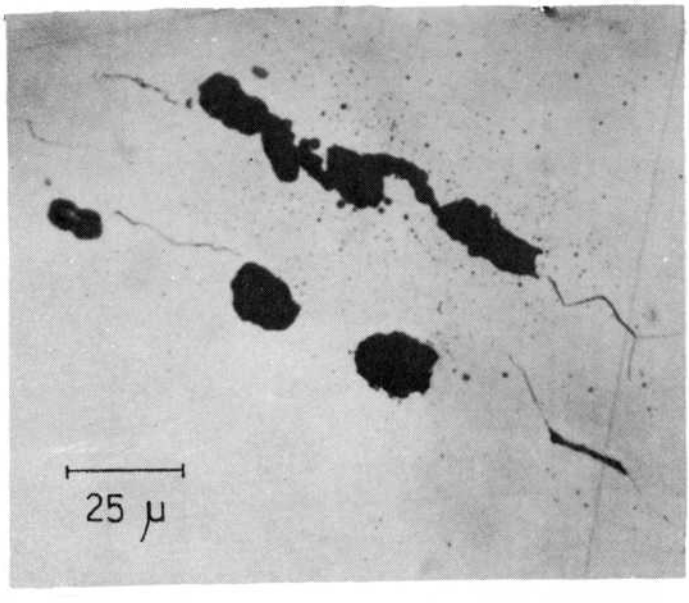

Fig.39- Fissures initiating at pits. AISI 4340 steel in deaerated 0.5M NaCl solution at 25ºC. E= -0.24V(nhe). Galvele and Semino (57).

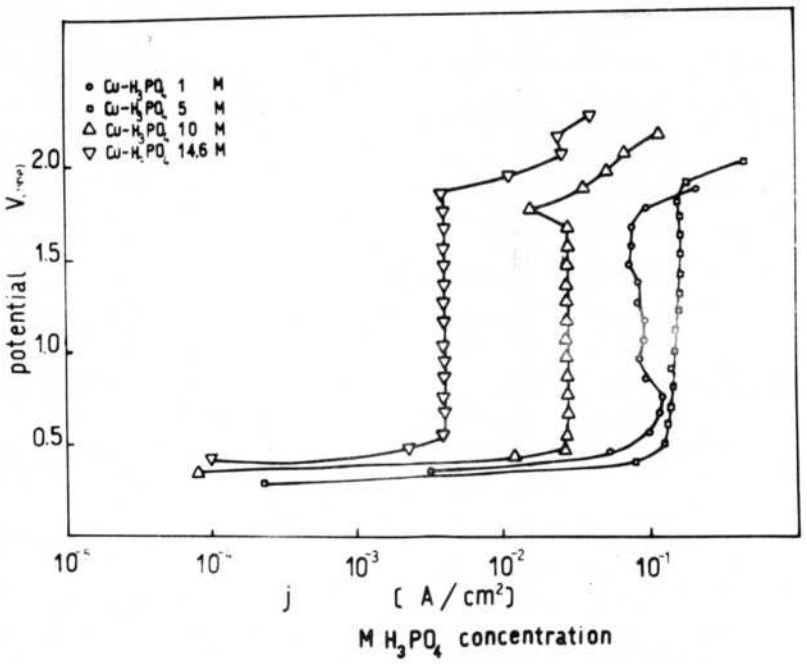

Fig.40- Potentiostatic polarization curves for pure Cu in deaerated H_3PO_4 solutions, at 25ºC.

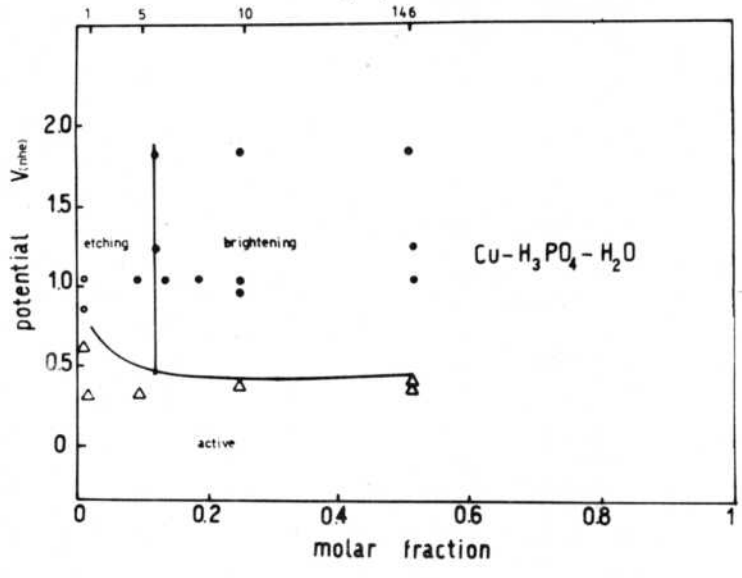

Fig.41- Potential/Molar Fraction diagram for Cu-H_3PO_4-H_2O, at 25ºC.

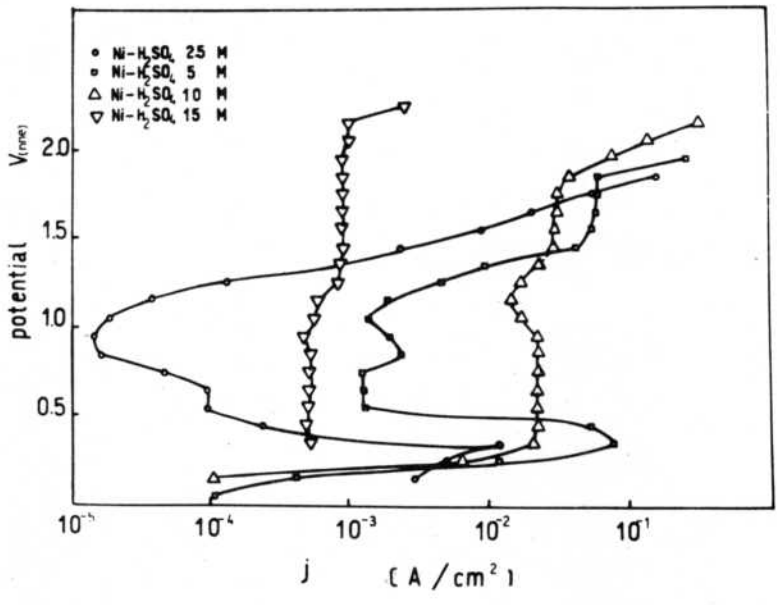

Fig.42- Potentiostatic polarization curves for Ni in deaerated H_2SO_4 solutions at 25ºC.

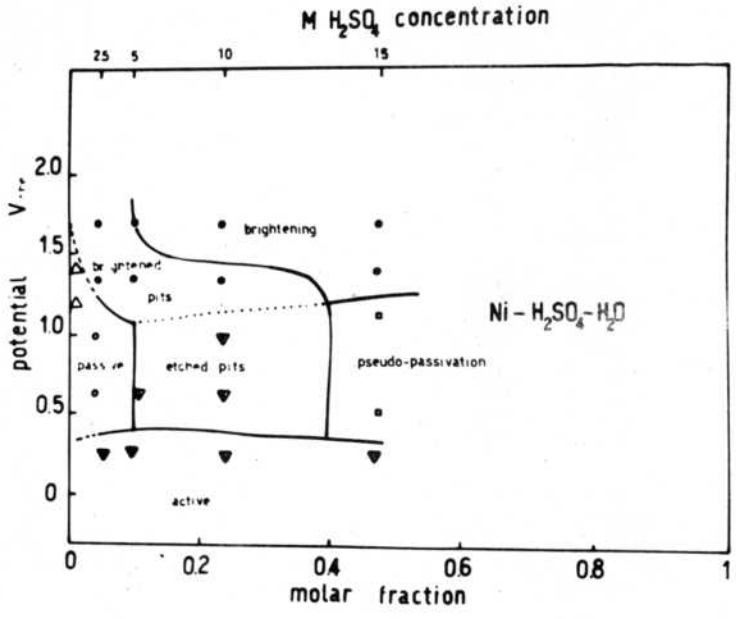

Fig.43- Potential/Molar Fraction diagram for Ni-H_2SO_4-H_2O at 25ºC.

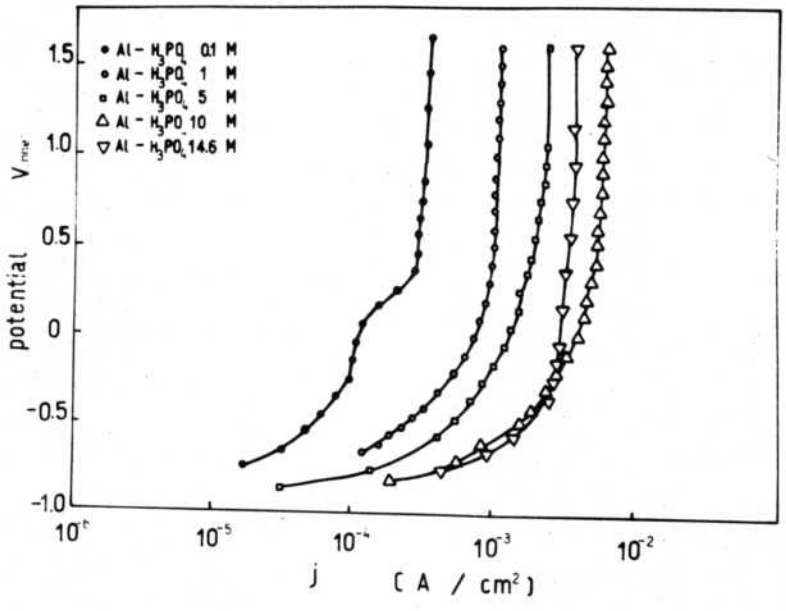

Fig.44- Potentiostatic polarization curves for Al in deaerated H_3PO_4 solutions, at 25ºC.

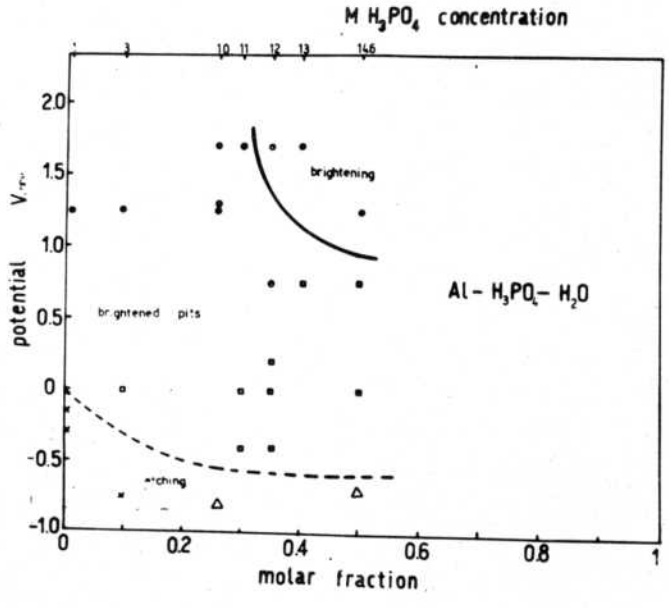

Fig.45- Potential/Molar Fraction diagram for Al-H_3PO_4-H_2O at 25ºC.